



Study of Higgs boson pair production in the HH \rightarrow bby final state with 308 fb⁻¹ of data collected at $\sqrt{s}=13$ TeV and 13.6 TeV by ATLAS experiment

Yong Zhou Nanjing University

arXiv:2507.03495

CLHCP 2025

Xinxiang, Henan, China

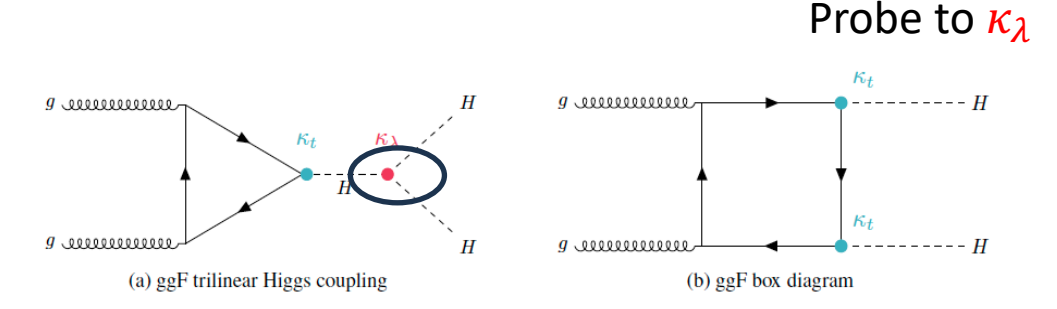
Motivation

The Higgs potential describes the self-interaction of the Higgs field and governs electroweak symmetry breaking(EWSB).
 After EWSB, the Higgs potential is given by:

$$V(\phi) = \frac{1}{2} m_H H^2 + \frac{\lambda_3}{4} v H^3 + \frac{\lambda_4}{4} H^4$$
 (In the SM , $v \approx 246 GeV$, $m_H \approx 125 GeV$, $\lambda_3 = \lambda_4 = \lambda_{SM} = \frac{m_H}{2v^2} \approx 0.13$)

• Searching for di-Higgs production is the **unique experimental** means to **directly probe** the Higgs trilinear self coupling $(\kappa_{\lambda} = \frac{\lambda_{3}, \text{obs}}{\lambda_{SM}})$.

> Non-resonant HH production

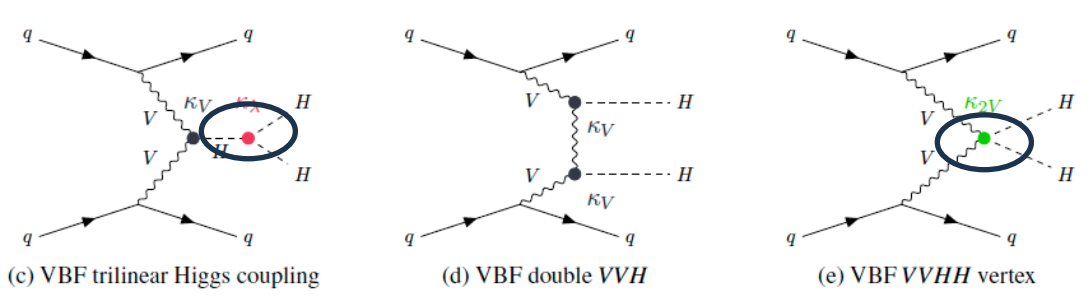


Gluon-gluon fusion(ggFHH)

$$\sigma_{HH}^{ggF} = 30.77 \text{ fb } @ 13 \text{ TeV}$$

 $\sigma_{HH}^{ggF} = 34.13 \text{ fb } @ 13.6 \text{ TeV}$

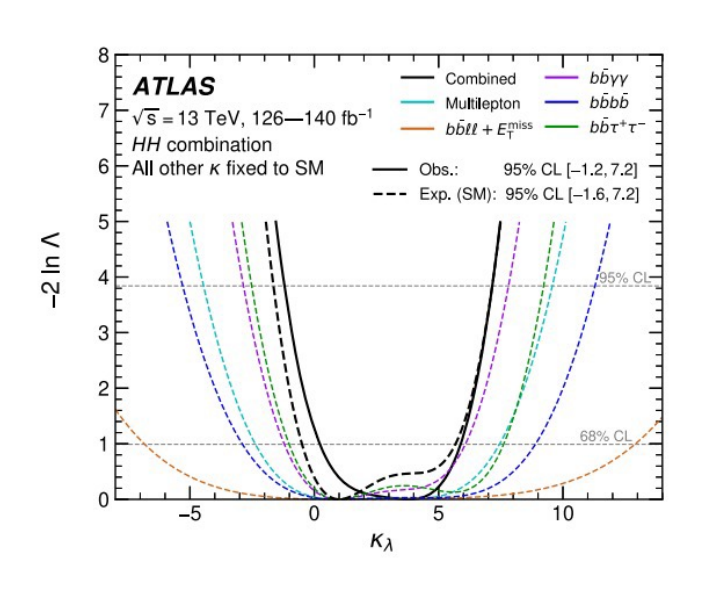
Unique probe to κ_{2V}

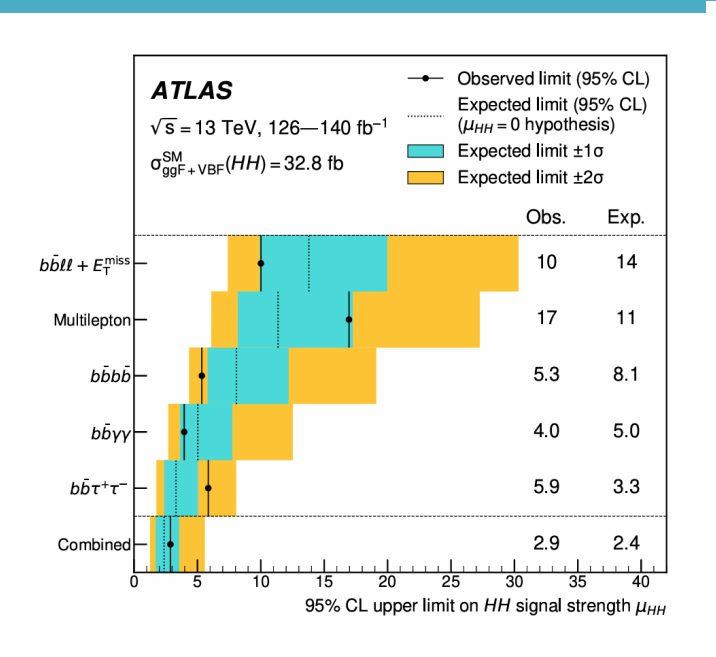


Vector boson fusion(VBFHH)

$$\sigma_{HH}^{VBF} = 1.69 \text{ fb} @ 13 \text{ TeV} \sigma_{HH}^{VBF} = 1.87 \text{ fb} @ 13.6 \text{ TeV}$$

$HH \rightarrow bb\gamma\gamma$ channel



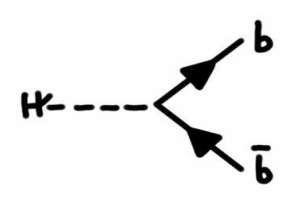


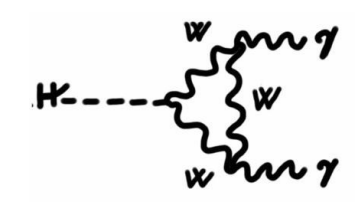
bb ww ZZ ττ ΥΥ bb 34% ww 25% 4.6% ττ 7.3% 2.7% 0.39% ZZ 3.1% 1.1% 0.33% 0.069% 0.26% 0.10% 0.028% 0.012% 0.0005% ΥΥ

Run2 Combination (PhysRevLett.133.101801)

- HH $\rightarrow bb\gamma\gamma$ channel is one of the golden channels in HH combination
- HH $\rightarrow bb\gamma\gamma$ final state:
 - ✓ Highest branching ratio (59%)
 - x Large QCD background.
 - x Very Low branching ratio(0.23%)
 - **✓ Excellent photon trigger and reconstruction efficiency**
 - \checkmark Excellent $m_{\gamma\gamma}$ resolution(1-2GeV)







Data and MC sample

- **Data samples**: Full run2($140fb^{-1}$) + partial run3($168fb^{-1}$) dataset.
- Diphoton trigger are used for all years(negligible impact from single photon trigger)

Datasets & GRL

	luminosity (fb ⁻¹)	GRL
2015	3.24	
2015	3.24	data15_13TeV.periodAllYear_DetStatus-v89-pro21-02_Unknown_PHYS_StandardGRL_All_Good_25ns.xml
2016	33.40	data16_13TeV.periodAllYear_DetStatus-v89-pro21-01_DQDefects-00-02-04_PHYS_StandardGRL_All_Good_25ns.xml
2017	44.63	data17_13TeV.periodAllYear_DetStatus-v99-pro22-01_Unknown_PHYS_StandardGRL_All_Good_25ns_Triggerno17e33prim.xml
2018	58.79	data18_13TeV.periodAllYear_DetStatus-v102-pro22-04_Unknown_PHYS_StandardGRL_All_Good_25ns_Triggerno17e33prim.xml
2022	31.39	data22_13p6TeV.periodAllYear_DetStatus-v109-pro28-04_MERGED_PHYS_StandardGRL_All_Good_25ns_igmore_TRIGMUO_TRIGLAR.xml
2023	27.23	data23_13p6TeV.periodAllYear_DetStatus-v110-pro31-06_MERGED_PHYS_StandardGRL_All_Good_25ns_ignoreTRIG_JETCTPIN.xml
2024	109.4	physics_25ns_data24.xml

Triggers

	trigger
2015	HLT_g35_loose_g25_loose
2016	HLT_g35_loose_g25_loose
2017	HLT_g35_medium_g25_medium_L12EM20VH
2018	HLT_g35_medium_g25_medium_L12EM20VH
2022	HLT_g35_medium_g25_medium_L12EM20VH
2023	HLT_g35_medium_g25_medium_L12eEM24L
2024	HLT_g35_medium_g25_medium_L12eEM24L

MC samples

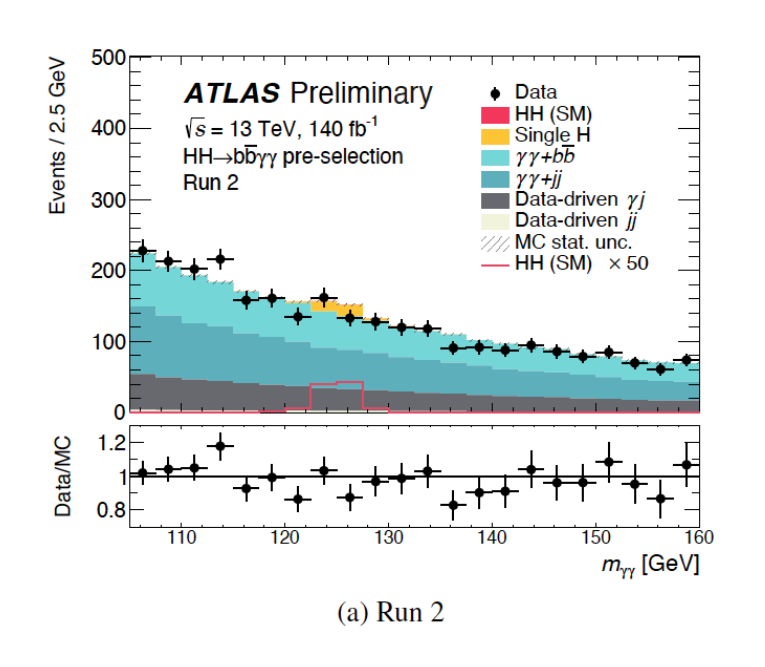
Process	Generator	PDF set	Showering	Tune	Accuracy	Order of σ calculation	
ggF <i>HH</i> VBF <i>HH</i>	Powheg Box v2 [59–63] MadGraph5_aMC@NLO [65]	PDF4LHC21 [64] NNPDF3.0 _N Lo [66]	Рутніа 8.309 [67] Рутніа 8.309	A14 [68] A14	NLO LO	NNLO N³LO	HH signal
ggF H	NNLOPS [59-61, 69, 70]	PDF4LHC15nlo (PDF4LHC21)	Рутніа 8.309	AZNLO [71] (A14)	NNLO	N^3LO	
VBFH	Powheg Box v2 [59–61, 72]	PDF4LHC15nlo (PDF4LHC21)	Рутніа 8.309	AZNLO (A14)	NLO	NNLO	
WH	Powheg Box v2 [59-61, 73]	PDF4LHC15nlo (PDF4LHC21)	Рутніа 8.309	AZNLO (A14)	NLO	NNLO	
$qq \rightarrow ZH$	Powheg Box v2 [59-61, 73]	PDF4LHC15nlo (PDF4LHC21)	Рутніа 8.309	AZNLO (A14)	NLO	NNLO	Single H
$gg \rightarrow ZH$	Powheg Box v2 [59-61, 73]	PDF4LHC15nlo (PDF4LHC21)	Рутніа 8.309	A14	LO	NLO	
$t \bar{t} H$	Powheg Box v2 [59-61, 74]	NNPDF3.0nlo (PDF4LHC21)	Рутніа 8.309	A14	NLO	NNLO	Single H background
$bar{b}H$	Powheg Box v2 [59–61, 75]	NNPDF3.0nlo (PDF4LHC21)	Рутніа 8.309	A14	NLO	NNLO	baokg. carra
tHq	MadGraph5_aMC@NLO	NNPDF3.0nlo	Рутніа 8.309	A14	NLO	NLO	
tHW	MadGraph5_aMC@NLO	NNPDF3.0nlo	Рутніа 8.309	A14	NLO	NLO	
γγ+jets	Sherpa 2.2.14 [76]	NNPDF3.0nnlo	Sherpa 2.2.14	_	_	_	Continuum
$\gamma\gamma bar{b}$	Sherpa 2.2.14	NNPDF3.0nnlo	Sherpa 2.2.14	-	_	_	b a alcomound
-							background

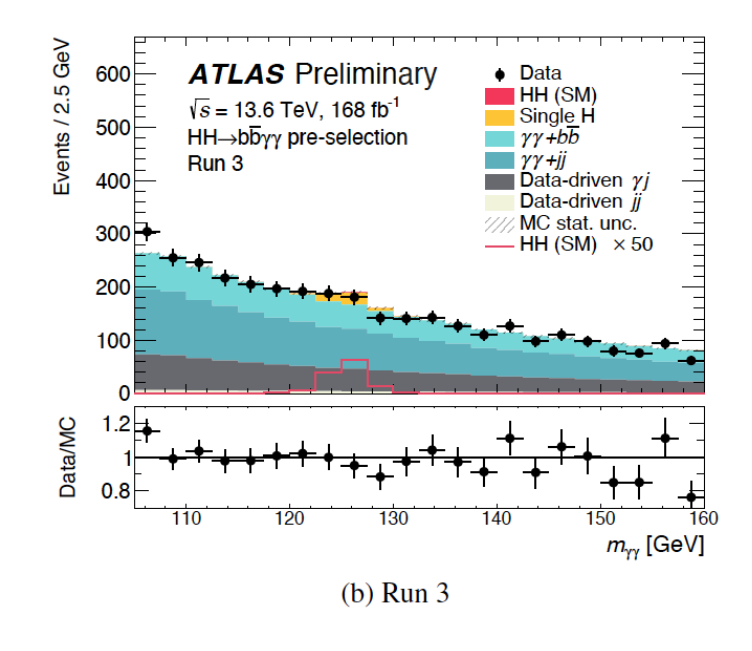
ggFHH:SM+5BSM sample

VBFHH:SM+12BSM sample

Pre-Selection

$H o \gamma \gamma$ Selection	H o bb Selection	ttH reduction	
• 2 tight and isolated photons $p_T/m_{\gamma\gamma}>0.35(0.25) \text{ for leading (sub-leading) photon.}$ • 105 GeV< $m_{\gamma\gamma}$ <160 GeV .	• $N_{b-jets} \ge 2$ at GN2 85% WP • μ -in-jet+ p_T -Reco Correction • Kinematic Fit.	• $N_{lep} = 0$ • $N_{central jets} < 6$	





Selection	Yields	Entries	Efficiency [%]	Cumul. Eff. [%]
All events	11.40	1,580,000	100.00	100.00
event clean and dalitz filter	11.33	1,570,299	99.38	99.38
Pass trigger	7.00	971,617	61.78	61.39
2 loose photons	6.35	882,345	90.75	55.71
trigger matching	6.31	877,171	99.42	55.39
2 tight ID photon	5.55	772,417	87.93	48.71
2 tight ID and Iso photons	4.99	695,346	89.88	43.78
rel. pT cuts	4.58	639,762	91.87	40.22
myy in [105,160]GeV	4.58	639,030	99.88	40.17
Nlep = 0	4.56	636,918	99.66	40.04
at least 2 Nj	4.03	563,660	88.25	35.33
Nj central<6	3.94	550,899	97.75	34.54
At least 2 b-jets with 85% WP	1.96	276,953	49.89	17.23
T 11 11 C (C C	TITI	Б : 1	1 (0) () 4 E0	: D 0

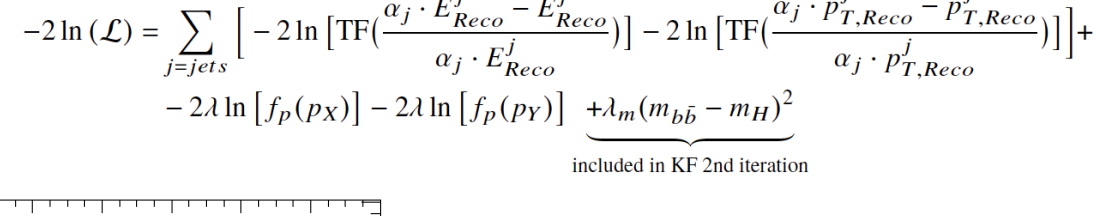
Table 11: Cutflow for HH ggF signal sample (SM) - AF3 in Run2.

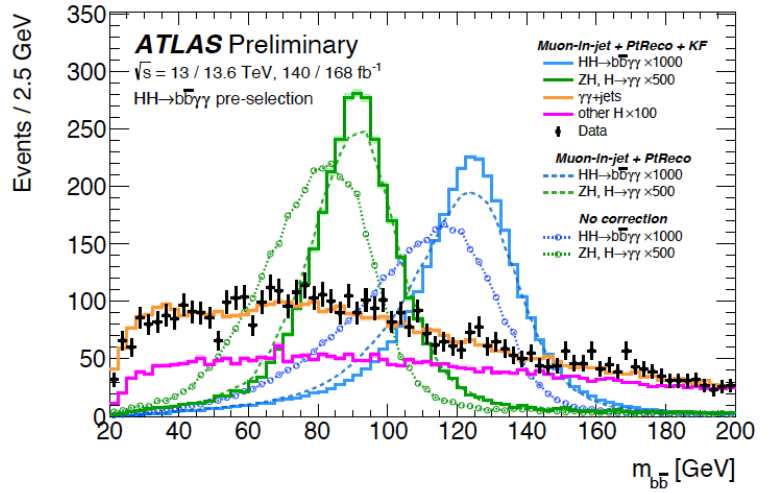
Kinematic Fit

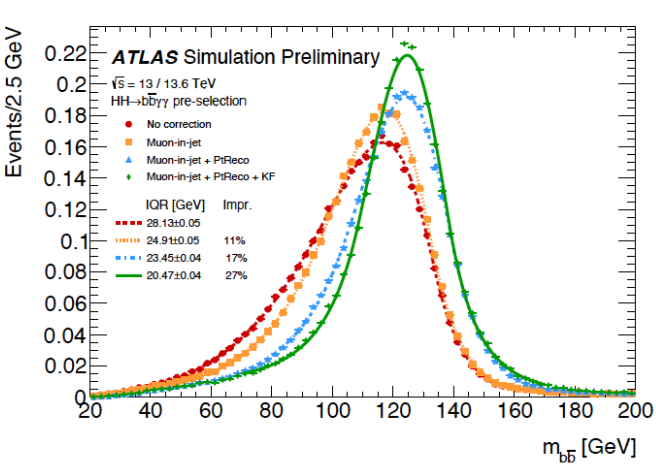
- The Kinematic Fit is an event-by-event correction to calibrate the HH system in the transverse plane by using the $H \to \gamma \gamma$ system to balance the $H \rightarrow bb$ system.
- The KF using log-likelihood minimization, The likelihood function contains two iterations and defined by:

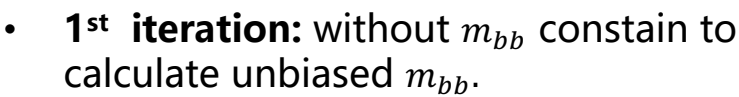
$$-2\ln(\mathcal{L}) = \sum_{j=jets} \left[-2\ln\left[TF\left(\frac{\alpha_{j} \cdot E_{Reco}^{j} - E_{Reco}^{j}}{\alpha_{j} \cdot E_{Reco}^{j}}\right) \right] - 2\ln\left[TF\left(\frac{\alpha_{j} \cdot p_{T,Reco}^{j} - p_{T,Reco}^{j}}{\alpha_{j} \cdot p_{T,Reco}^{j}}\right) \right] \right] +$$

$$-2\lambda \ln\left[f_{p}(p_{X}) \right] - 2\lambda \ln\left[f_{p}(p_{Y}) \right] + \lambda_{m} (m_{b\bar{b}} - m_{H})^{2}$$
included in KE 2nd its extraction

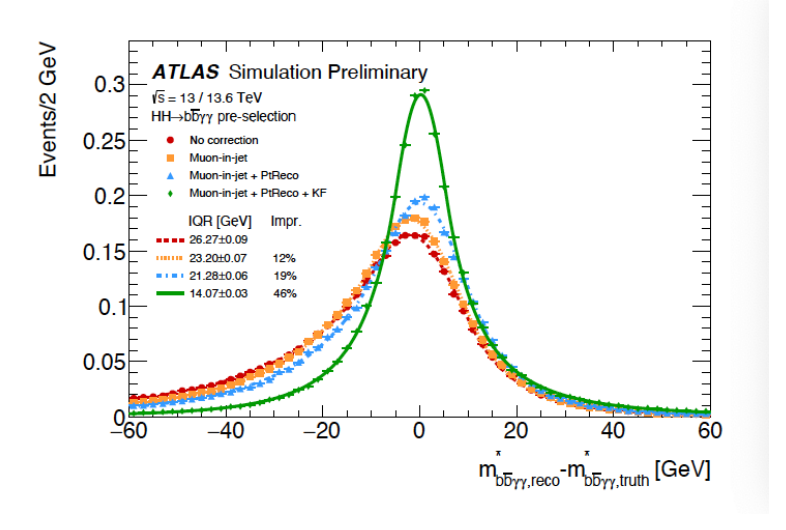








2nd iteration: with m_{hh} constrain to improve the $m_{bb\nu\nu}$ resolution.



The KF improved the m_{bb} and m_{bbvv} resolutions by 27%(13%) and 46%(33%) with respect to No correction(bjet calibration).

Event classification

- The modified invariant mass $(m_{bb\gamma\gamma}^* = m_{bb\gamma\gamma} (m_{bb} 125 GeV) (m_{\gamma\gamma} 125 GeV)$) is used to split the events into **High** mass region $(m_{bb\gamma\gamma}^* > 350 GeV$, target SM signal) and **Low mass region** $(m_{bb\gamma\gamma}^* < 350 GeV$, target BSM signal).
- In each region. A dedicated BDT model is trained by combining the run2 and run3 MC sample using XGboost.

Variable	Definition
Photon candidates	
$p_{\mathrm{T}}/m_{\gamma\gamma}$	Transverse momentum of each photon divided by the di-photon invariant mass $m_{\gamma\gamma}$
η and ϕ	Pseudorapidity and azimuthal angle of each photon
$\Delta R(\gamma_1, \gamma_2)$	Angular distance between the two photons
b-jet candidates	
b-tag status	Tightest fixed b-tag working point (60%, 70%, 77%, 85%) that each jet fulfills
p_{T}, η and ϕ	Transverse momentum, pseudorapidity and azimuthal angle of each jet
$p_{\mathrm{T}}^{bar{b}},\eta_{bar{b}}$ and $\phi_{bar{b}}$	Transverse momentum, pseudorapidity and azimuthal angle of the two-b-jet system
$\Delta R(b_1, b_2)$	Angular distance between the two b -jets
$m_{bar{b}}$	Invariant mass of the two b -jets
Single topness	Variable used to identify $t \to Wb \to q\bar{q}'b$ decays. For the definition, see Ref. [JHEP 01 (2024) 066].
Other jets (only first two, if present, ranked	by discrete b-tagging score)
b-tag status	Tightest fixed b-tag working point that each jet fulfills
p_{T}, η and ϕ	Transverse momentum, pseudorapidity and azimuthal angle of each jet
VBF-jet candidates	
$\Delta \eta_{jj}, m_{jj}$	Pseudorapidity difference and invariant mass of the two jets
Event-level variables	
Transverse sphericity, planar flow, p_T balance	For the definitions, see Refs. [EPJC 72 2211, PRD 79 074017, JHEP 01 (2024) 066]
H_{T}	Scalar sum of the p_T of the jets in the event
$E_{\mathrm{T}}^{\mathrm{miss}}$ and ϕ^{miss}	Missing transverse momentum and its azimuthal angle
*	The four-body invariant mass of the two photons and two b -jets,
$m^*_{bar{b}\gamma\gamma}$	$m_{b\bar{b}\gamma\gamma}^* = m_{b\bar{b}\gamma\gamma} - (m_{b\bar{b}} - 125 \text{ GeV}) - (m_{\gamma\gamma} - 125 \text{ GeV})$

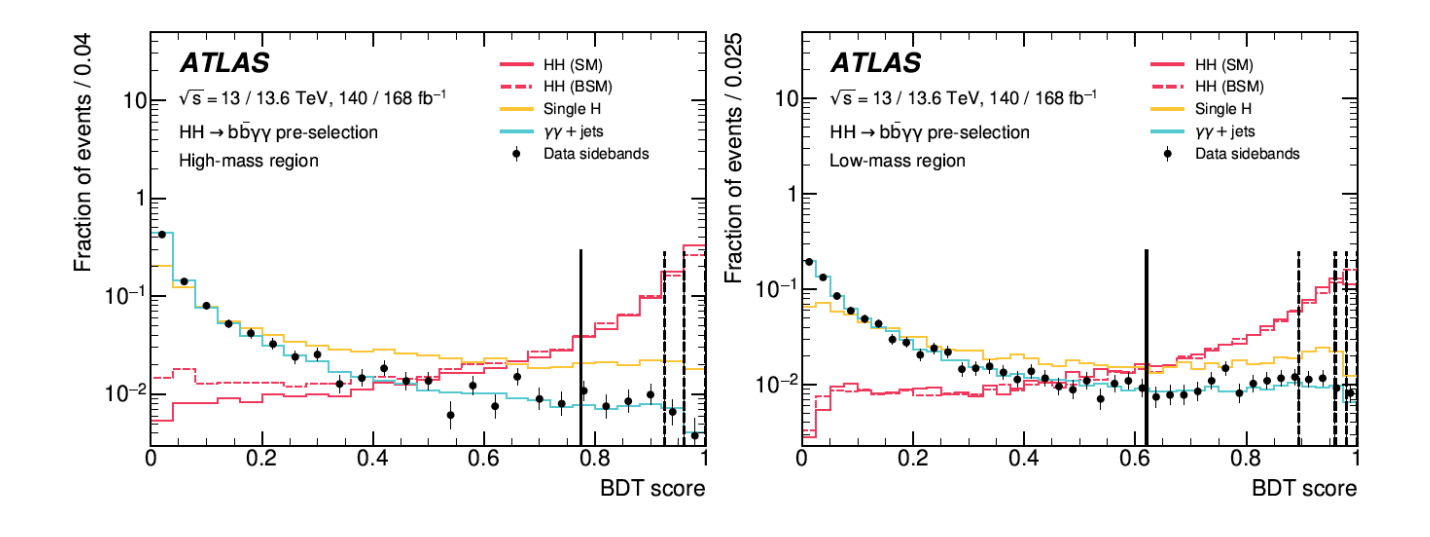
Training and test samples					
Low $m_{b\bar{b}\gamma\gamma}^*$ region	High $m^*_{b\bar{b}\gamma\gamma}$ region				
Target signal					
ggF HH					
$\kappa_{\lambda} = 10, 5$	$\kappa_{\lambda} = 1$				
VBF HH					
$ \kappa_{\lambda} = 0, \kappa_{2V} = 1, \kappa_{V} = 1 $	$\kappa_{\lambda} = 1$, $\kappa_{2V} = 1$, $\kappa_{V} = 1$				
$ \kappa_{\lambda} = 1, \kappa_{2V} = 1.5, \kappa_{V} = 1 $	$ \kappa_{\lambda} = 0, \kappa_{2V} = 1, \kappa_{V} = 1 $				
$ \kappa_{\lambda} = 1, \kappa_{2V} = 3, \kappa_{V} = 1 $	$\kappa_{\lambda} = 1$, $\kappa_{2V} = 1.5$, $\kappa_{V} = 1$				
$\kappa_{\lambda} = -5, \kappa_{2V} = 1, \kappa_{V} = 0.5$	$\kappa_{\lambda} = 1$, $\kappa_{2V} = 3$, $\kappa_{V} = 1$				
$\kappa_{\lambda} = 10, \kappa_{2V} = 1, \kappa_{V} = 1$	$\kappa_{\lambda} = -5$, $\kappa_{2V} = 1$, $\kappa_{V} = 0.5$				
	$ \kappa_{\lambda} = 10, \kappa_{2V} = 1, \kappa_{V} = 1 $				
Background					
ggF H , VBF H , $W^{\pm}H$, $b\bar{b}H$, $qq \rightarrow ZH$, $gg \rightarrow ZH$, $tHjb$, tWH , $t\bar{t}H$, $\gamma\gamma$ +jets					
Sample split					
Training	event_number % $4 \le 1$				
Validation (during training)	<pre>event_number % 4 == 2</pre>				
Test	<pre>event_number % 4 == 3</pre>				

Event Categorization

- The event categories are defined based on the HM and LM BDT score distributions. 3HM and 4 LM categories are extracted for Run2 and Run3 separately:
 - The category boundaries are determined by maximizing the number-counting significance:

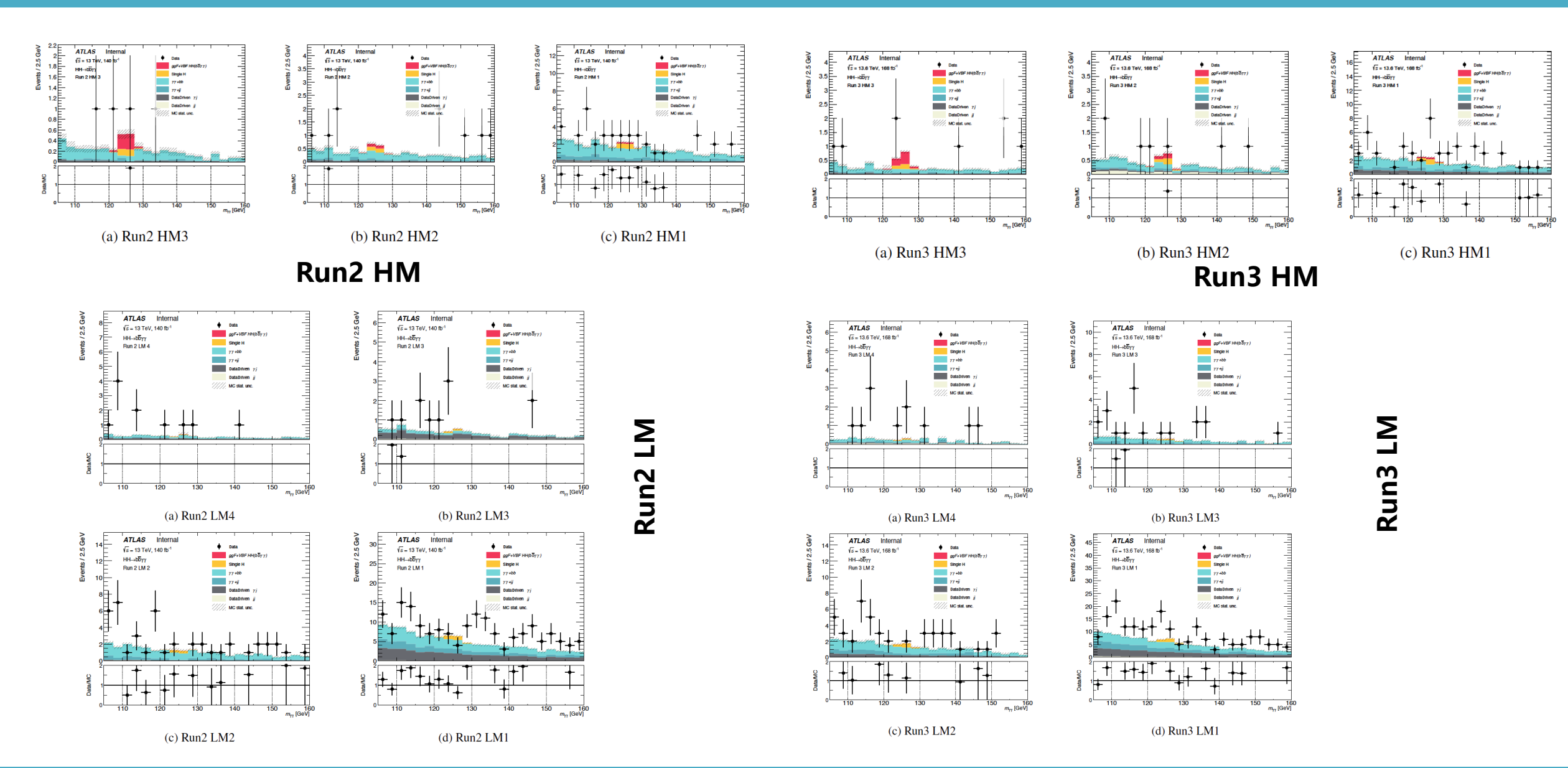
$$Z_{cat} = \sqrt{2[(S+B).\log(1+\frac{S}{B})-S]}$$
, $Z_{tot} = \sqrt{\sum_{cat} Z_{cat}^2}$

- Requiring at least 11 $\gamma\gamma + jets$ events for each sub category to ensure enough events for background modeling.
- The same boundaries score are applied for Run2 and Run3 separately. (14 categories in total)



Category	Selection criteria
High Mass 1	$m_{b\bar{b}\gamma\gamma}^* \ge 350 \text{ GeV}, \text{BDT score} \in [0.775, 0.925]$
High Mass 2	$m_{b\bar{b}\gamma\gamma}^* \ge 350 \text{ GeV}, \text{BDT score} \in [0.925, 0.960]$
High Mass 3	$m_{b\bar{b}\gamma\gamma}^* \ge 350 \text{ GeV}, \text{BDT score} \in [0.960, 1.000]$
Low Mass 1	$m_{b\bar{b}\gamma\gamma}^* < 350 \text{ GeV}, BDT \text{ score} \in [0.620, 0.895]$
Low Mass 2	$m_{b\bar{b}\gamma\gamma}^* < 350 \text{ GeV}, BDT \text{ score} \in [0.895, 0.960]$
Low Mass 3	$m_{b\bar{b}\gamma\gamma}^* < 350 \text{ GeV}, \text{BDT score} \in [0.960, 0.980]$
Low Mass 4	$m_{b\bar{b}\gamma\gamma}^* \ge 350 \text{ GeV}, \text{BDT score} \in [0.775, 0.925]$ $m_{b\bar{b}\gamma\gamma}^* \ge 350 \text{ GeV}, \text{BDT score} \in [0.925, 0.960]$ $m_{b\bar{b}\gamma\gamma}^* \ge 350 \text{ GeV}, \text{BDT score} \in [0.960, 1.000]$ $m_{b\bar{b}\gamma\gamma}^* < 350 \text{ GeV}, \text{BDT score} \in [0.620, 0.895]$ $m_{b\bar{b}\gamma\gamma}^* < 350 \text{ GeV}, \text{BDT score} \in [0.895, 0.960]$ $m_{b\bar{b}\gamma\gamma}^* < 350 \text{ GeV}, \text{BDT score} \in [0.960, 0.980]$ $m_{b\bar{b}\gamma\gamma}^* < 350 \text{ GeV}, \text{BDT score} \in [0.980, 1.000]$

Analysis Categories



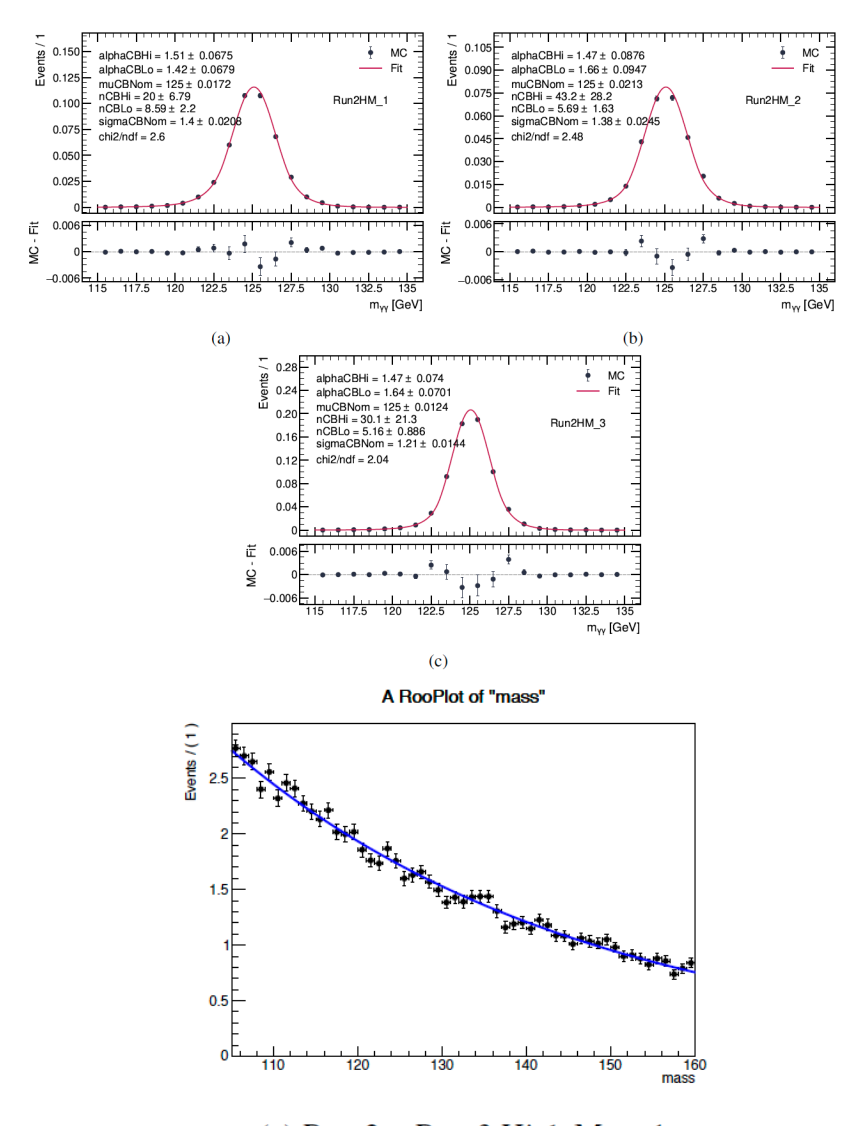
Signal and Background Modeling

Signal Modelling

- The $m_{\gamma\gamma}$ distribution of the di-Higgs signal and single Higgs background are modelled with a Double-side Crystal Ball (DSCB) function.
- The shape parameters are extracted by an unbinned likelihood fit to the SM ggF and VBF HH MC samples.
- The shape parameters are shared between di-Higgs signals and signal Higgs backgrounds for each categories.

Background Modelling

- Single H Modelling: DSCB function, the same shape parameter as HH.
- Continuum background Modelling:
 - The continuum background is modelled using an exponential function: $N_{bkg} \cdot \exp(-\beta m_{\gamma\gamma})$.
 - The exponential slopes are the same for each Run2 and Run3 category
 pair, while the normalization of backgrounds are determined separately in
 the final fit(7 slope+14 Norm).



(a) Run 2 + Run 3 High Mass 1

Systematic Uncertainties

- The systematic uncertainties are mainly relevant for the HH signal and resonant background.
- The spurious signal uncertainties are the only source of uncertainties relevant for continuum background.

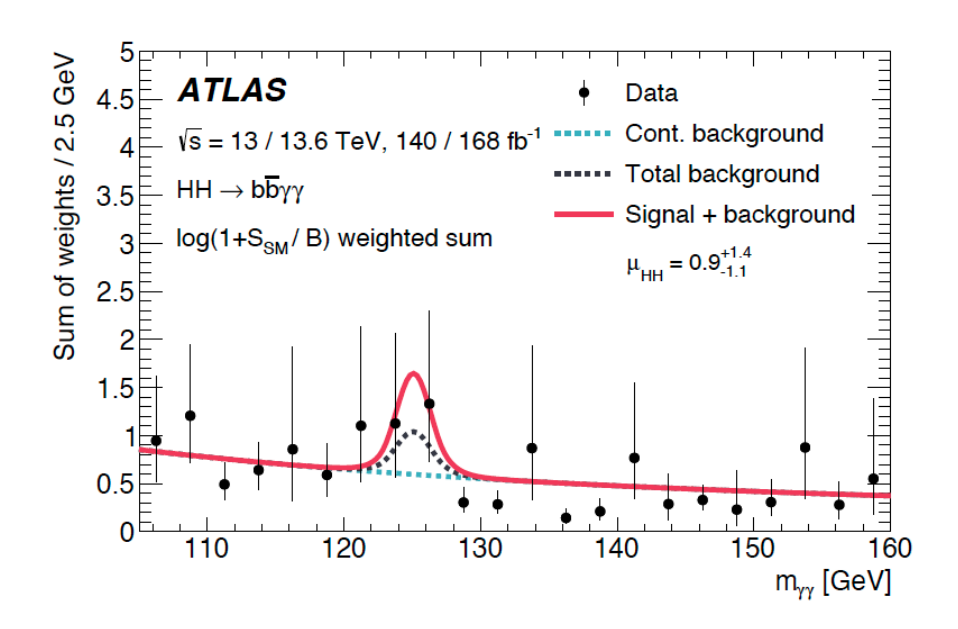
> Correlation Scheme:

- Trigger: Uncorrelated between run2 and run3. The decorrelation between 2022 and 2023/2024 due to L1 trigger change.
- JetMet: Partial correlated.
- Muon ,theory, spurious uncertainties: full correlated
- The Rest of experimental uncertainties are uncorrelated.
- The total uncertainty still dominant by statistical uncertainty

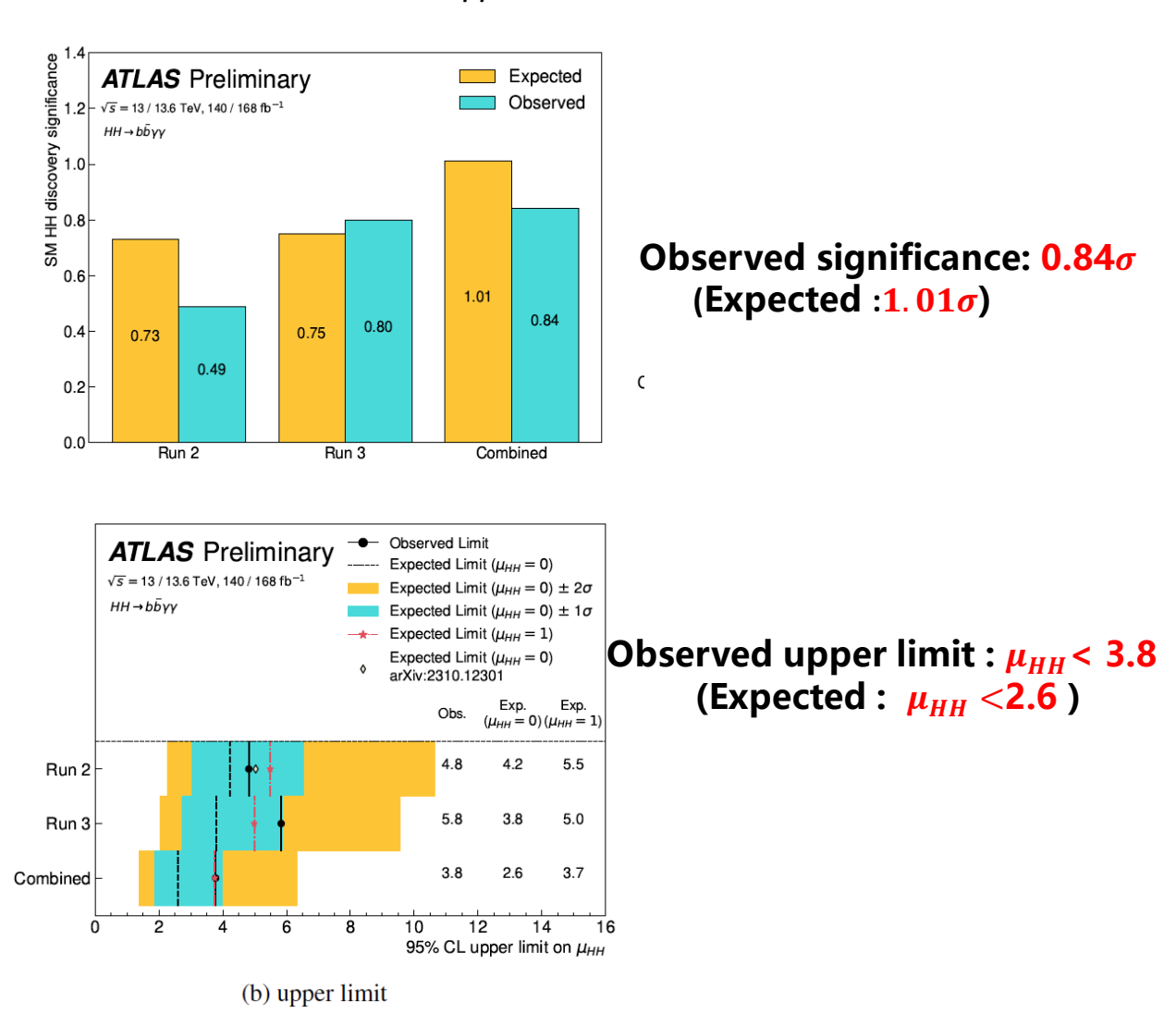
	Relative impact [%		
Source of systematic uncertainty	Up	Down	
Experimental			
Photon energy scale	+20	-30	
Photon energy resolution	+13	-6.8	
Photon efficiency	+13	-2.5	
Jet	+9.6	-6.4	
Luminosity	+6.3	-1.1	
Theory			
QCD scale + m_{top} , PDF+ α_S	+34	-4.5	
$\mathcal{B}(H \to \gamma \gamma, b\bar{b})$	+9.9	-2.1	
Parton showering model	± .	15	
Heavy-flavour content	±2	29	
Background model			
Spurious signal	±0	6.5	

Results

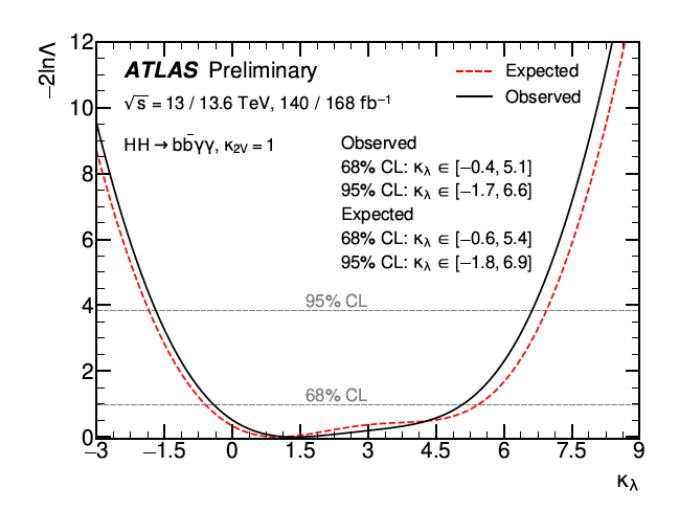
• The results are extracted from a simultaneous profile-likelihood fit to the $m_{\gamma\gamma}$ distribution in all categories.

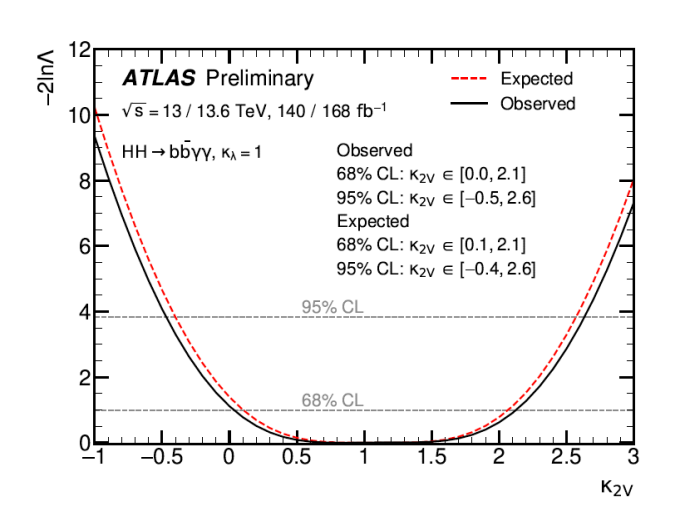


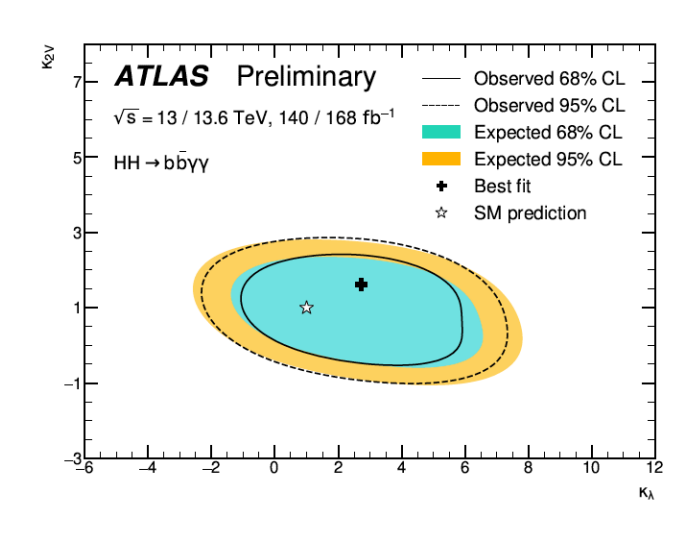
"Weighted" plot of $m_{\gamma\gamma}$ by summing the contribution for each category and weighting for each contribution with $w_c = \log(1 + \frac{S_c}{B_c})$.



Results







	Run 2		Run 3		Combined	
	observed	expected	observed	expected	observed	expected
μ_{HH}	0.6+1.8	1+2.1	1.4+2.2	1 ^{+1.9} _{-1.3}	0.9+1.4	1 ^{+1.3} _{-1.0}
κ _λ (68% CI)	[-0.2, 4.3]	[-1.2, 6.3]	[-1.5, 7.1]	[-1.0, 6.0]	[-0.4, 5.1]	[-0.6, 5.4]
κ _λ (95% CI)	[-1.8, 6.4]	[-2.9, 8.0]	[-3.3, 8.5]	[-2.6, 7.7]	[-1.7, 6.6]	[-1.8, 6.9]
κ _{2V} (68% CI)	[-0.2, 2.4]	[-0.2, 2.3]	[-0.2, 2.3]	[-0.1, 2.2]	[0.0, 2.1]	[0.1, 2.1]
κ _{2V} (95% CI)	[-0.9, 3.1]	[-0.9, 3.0]	[-0.8, 3.0]	[-0.7, 2.9]	[-0.5, 2.6]	[-0.4, 2.6]

- Observed κ_{λ} constrain at 95% CL: [-1.7,6.6] (Expected:[-1.8,6.9])
- Observed κ_{2V} constrain at 95% CL: [-0.5,2.6] (Expected: [-0.4,2.6])

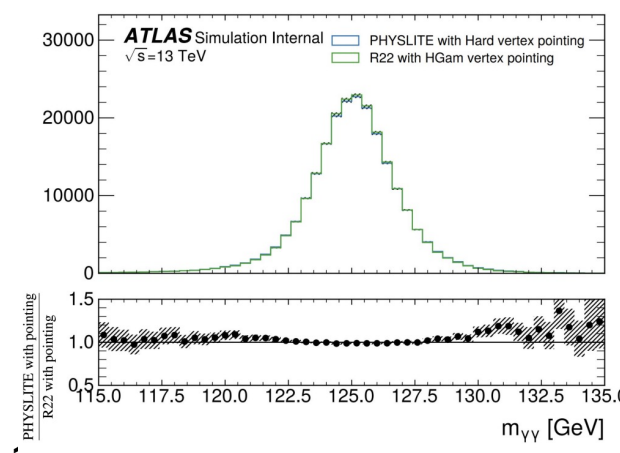
Summary

- Search for Non-resonant HH Pair Production in $bb\gamma\gamma$ final state with full run2 and partial run3 dataset is presented
 - First ATLAS analysis with more than 300 fb^{-1} dataset
- The Analysis strategy has been improved in multiple ways over the previous analysis
 - ➤ Addition of 168 fb⁻¹ data from Run3
 - > GN2 for b-tagging and relaxing the number of b-jet requirement
 - \triangleright Kinematic Fit for improve the m_{bb} resolution
 - ➤ Tighter category cuts with Run2+3 combination
- Relative improvement with respect to previous analysis :
 - ✓ Expected upper limit on μ_{HH} improved by ~100%
 - ✓ Expected κ_{λ} constrain at 95% CL improved by ~20%
 - ✓ Expected κ_{2V} constrain at 95% CL improved by ~30%

Backup

Difference with respect to legacy analysis

- Production Framework : HGamCore → Easyjet(common HH fwk):
 - DAOD derivation : HIGG1D1 → PHYSLITE
 - Primary vertex: NN vertex \rightarrow Hardest vertex(highest track $\sum p_T^2$).



- b-tagging algorithm : DL1r → GN2:
 - GN2 has much better background rejection power compare to DL¹1.
 - Relax the b-jet requirements: b-tag WP 77% \rightarrow 85% and $N_{b-jet}=2$ \rightarrow $N_{b-jet}\geq 2$.
- Other changes and improvements:
 - Adopt the **Kinematic Fit** method to further improve the m_{bb} resolution.
 - Additional partial Run3 dataset: 2022 2024 data(168fb⁻¹).
 - MC generator and PDF set update
 - Retrain the BDT model and background shape correlation.
 - Powheg bug fixed,AF3,CP recommendations...

MC samples

603559	SM ggF HH ($\kappa_{\lambda}=$ 1)	FS+AF3
603558	ggF HH $\kappa_{\lambda} = 0$	AF3
603560	ggF HH $\kappa_{\lambda}^{\frown}=$ 5	AF3
603697	ggF HH $\kappa_{\lambda} = -1$	AF3
603695	ggF HH $\kappa_{\lambda}^{-}=$ 2.5	AF3
603696	ggF HH $\stackrel{\frown}{\kappa_{\lambda}}=$ 10	AF3
525376	SM VBF HH ($\kappa_{\lambda}=$ 1, $\kappa_{2V}=$ 1, $\kappa_{V}=$ 1)	FS+AF3
525377	VBF HH $\kappa_{\lambda}=$ 0, $\kappa_{2V}=$ 1, $\kappa_{V}=$ 1	AF3
525378	VBF HH $\kappa_{\lambda}^{\frown}=$ 2, $\kappa_{2V}^{\mathbf{-1}}=$ 1, $\kappa_{V}^{\mathbf{-1}}=$ 1	AF3
525379	VBF HH $\kappa_{\lambda}=$ 10, $\kappa_{2V}=$ 1, $\kappa_{V}=$ 1	AF3
525380	VBF HH $\hat{\kappa_{\lambda}}=1,~\kappa_{2V}=0,~\kappa_{V}=1$	AF3
525381	VBF HH $\kappa_{\lambda}=$ 1, $\kappa_{2V}=$ 0.5, $\kappa_{V}=$ 1	AF3
525382	VBF HH $\kappa_{\lambda}^{\cap}=$ 1, $\kappa_{2V}^{\mathbf{-1}}=$ 1.5, $\kappa_{V}^{\mathbf{-1}}=$ 1	AF3
525383	VBF HH $\stackrel{\frown}{\kappa}_{\lambda}=$ 1, $\stackrel{\frown}{\kappa}_{2V}=$ 2, $\kappa_{V}=$ 1	AF3
525384	VBF HH $\kappa_{\lambda}^{\frown}=$ 1, $\kappa_{2V}^{\mathbf{-}}=$ 3, $\kappa_{V}^{\mathbf{-}}=$ 1	AF3
525385	VBF HH $\kappa_{\lambda}=$ 1, $\kappa_{2V}=$ 1, $\kappa_{V}=$ 0.5	AF3
525386	VBF HH $\kappa_{\lambda} = 1, \ \kappa_{2V} = 1, \ \kappa_{V} = 1.5$	AF3
525387	VBF HH $\kappa_{\lambda}=$ 0, $\kappa_{2V}=$ 0, $\kappa_{V}=$ 1	AF3
525388	VBF HH $\kappa_{\lambda}=-$ 5, $\kappa_{2V}^{\mathbf{-}}=$ 1, $\kappa_{V}=$ 0.5	AF3
343981/602421	ggH	FS
346214/601482	VBF	FS
345318/601484	W^+H	FS
345317/601483	W^-H	FS
345319/601523	qq o ZH	FS
345061/601522	gg o ZH	FS
346525/602422	ttH	FS
345315/601710	ЬЬН	FS
545636	tHjb	FS
545639	tHW	FS
700980	$\gamma\gamma+$ 0,1(NLO),2,3(LO), $m_{\gamma\gamma}\in($ 90, 175 $)$ GeV	AF3
700711	$\gamma\gamma + b\bar{b}(NLO), m_{\gamma\gamma} \in (90, 175)$ GeV	AF3
		•

Objects definition

> Photons:

- Tight ID and FixedCutLoose Isolation.
- $|\eta| < 1.37$ or $1.52 < |\eta| < 2.37$.

> Jets:

- PFlow jets +Jet-Vertex Tagger(JVT) +FJVT.
- Anti-kt R = $0.4, p_T > 25 \ GeV, |\eta| < 4.5$
- b-tagging: GN2 with 85% WP + b-jet correction
- VBF jets(Additional jets except H \rightarrow bb candidate): the pair of jets with the highest m_{ij} .

> Leptons:

- Electrons: $p_T > 4.5~GeV$, $|\eta| < 1.37~or~1.52 < |\eta| < 2.37.Medium ID and Loose_VarRad Isolation.$
- Muons: $p_T > 3 \ GeV$, $|\eta| < 2.5$.Medium ID and pflowLoose_VarRad Isolation.

Overlap removal:

Use The common Athena OR instead of dedicate HGam OR (negligible impact)

Cutflow

Selection	Yields	Entries	Efficiency [%]	Cumul. Eff. [%]
All events	11.40	1,580,000	100.00	100.00
event clean and dalitz filter	11.33	1,570,299	99.38	99.38
Pass trigger	7.00	971,617	61.78	61.39
2 loose photons	6.35	882,345	90.75	55.71
trigger matching	6.31	877,171	99.42	55.39
2 tight ID photon	5.55	772,417	87.93	48.71
2 tight ID and Iso photons	4.99	695,346	89.88	43.78
rel. pT cuts	4.58	639,762	91.87	40.22
myy in [105,160]GeV	4.58	639,030	99.88	40.17
Nlep = 0	4.56	636,918	99.66	40.04
at least 2 Nj	4.03	563,660	88.25	35.33
Nj central<6	3.94	550,899	97.75	34.54
At least 2 b-jets with 85% WP	1.96	276,953	49.89	17.23

Table 11: Cutflow for HH ggF signal sample (SM) - AF3 in Run2.

Selection	Yields	Entries	Efficiency [%]	Cumul. Eff. [%]
All events	0.62	3,954,000	100.00	100.00
event clean and dalitz filter	0.62	3,915,533	99.02	99.02
Pass trigger	0.35	2,186,581	55.96	55.41
2 loose photons	0.31	1,959,665	89.56	49.63
trigger matching	0.31	1,945,370	99.27	49.27
2 tight ID photon	0.27	1,695,042	87.10	42.91
2 tight ID and Iso photons	0.24	1,514,105	89.34	38.34
rel. pT cuts	0.22	1,378,053	91.01	34.89
myy in [105,160]GeV	0.22	1,371,077	99.49	34.71
$N_{lep} = 0$	0.22	1,365,482	99.59	34.57
at least 2 N_j	0.21	1,299,181	95.15	32.90
N_j central<6	0.20	1,291,511	99.41	32.70
At least 2 b-jets with 85% WP	0.07	458,752	35.56	11.63

Table 12: Cutflow for HH VBF signal sample (SM) - AF3 in Run2.

Selection	Yields	Entries	Efficiency [%]	Cumul. Eff. [%]
All events	15.16	2,050,000	100.00	100.00
event clean and dalitz filter	14.96	2,023,037	98.68	98.68
Pass trigger	8.79	1,192,882	58.75	57.97
2 loose photons	8.11	1,101,256	92.30	53.51
trigger matching	8.05	1,093,066	99.26	53.11
2 tight ID photon	7.17	973,849	89.00	47.27
2 tight ID and Iso photons	6.51	886,484	90.88	42.96
rel. pT cuts	6.01	818,886	92.22	39.61
myy in [105,160]GeV	6.00	817,923	99.89	39.57
Nlep = 0	5.98	815,302	99.67	39.44
at least 2 Nj	5.28	721,369	88.27	34.81
Nj central<6	5.16	705,014	97.71	34.01
At least 2 b-jets with 85% WP	2.54	349,658	49.18	16.73

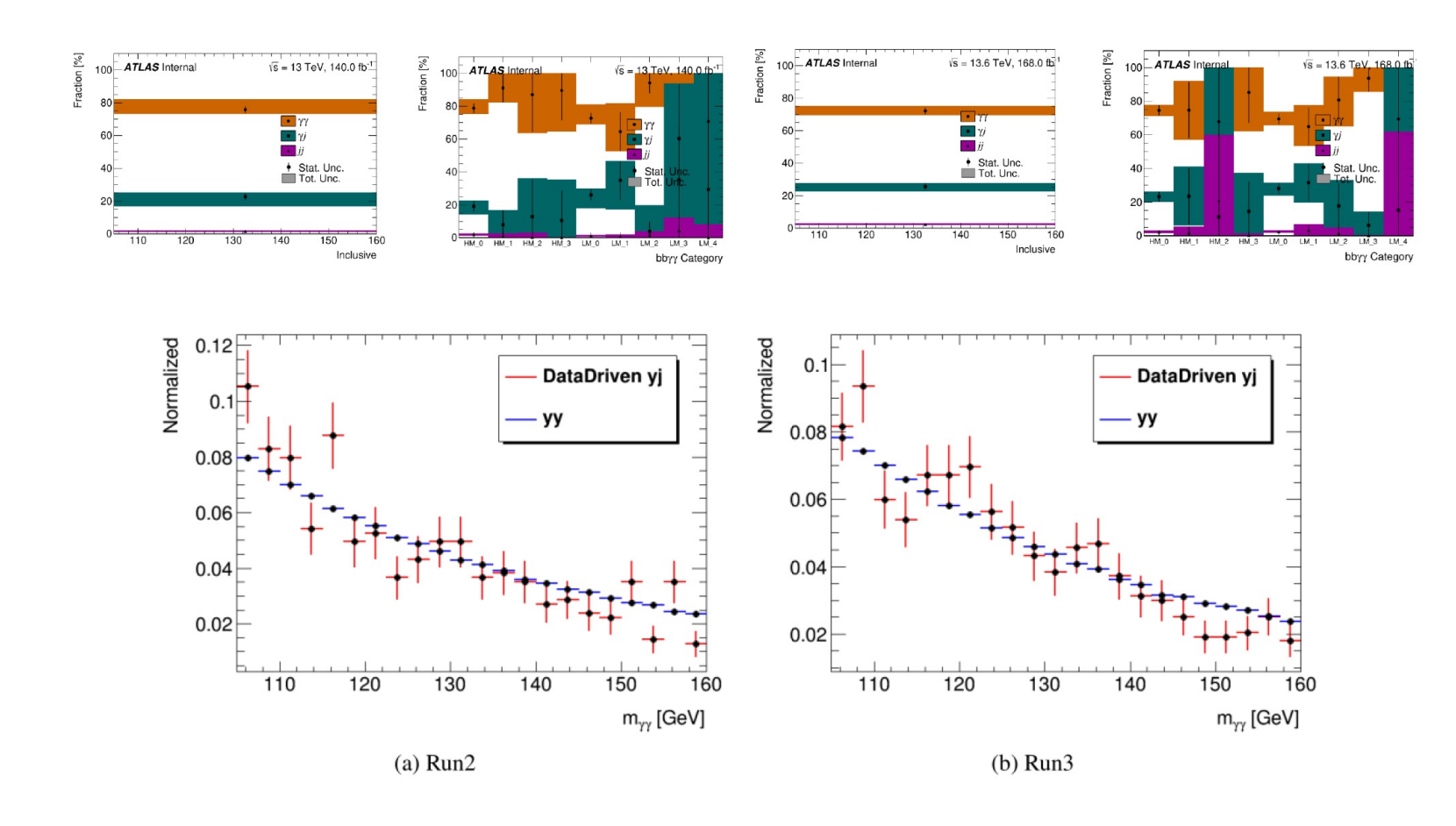
Table 13: Cutflow for HH ggF signal sample (SM) - AF3 in Run3

Selection	Yields	Entries	Efficiency [%]	Cumul. Eff. [%]
All events	0.83	440,000	100.00	100.00
event clean and dalitz filter	0.82	432,392	98.27	98.27
Pass trigger	0.43	228,934	53.00	52.08
2 loose photons	0.40	208,964	91.28	47.54
trigger matching	0.39	207,083	99.10	47.11
2 tight ID photon	0.34	181,855	87.82	41.37
2 tight ID and Iso photons	0.31	164,287	90.35	37.38
rel. pT cuts	0.28	150,088	91.34	34.14
myy in [105,160]GeV	0.28	149,303	99.48	33.97
Nlep = 0	0.28	148,755	99.63	33.84
at least 2 Nj	0.27	141,079	94.84	32.09
Nj central<6	0.27	140,222	99.39	31.90
At least 2 b-jets with 85% WP	0.09	48,219	34.41	10.98

Table 14: Cutflow for HH VBF signal sample (SM) - AF3 in Run3.

Background decomposition

- ABCD method on data sideband to estimate $\gamma\gamma$, γ + jet, jet + jet component
- similar shape between $\gamma\gamma$ and γ + jet



Hyperparameters

Hyperparameter	Range	Value for Low Mass BDT	Value for High Mass BDT
min child weight	[0,100]	27	84
colsample bytree	[0.3, 1]	0.64	0.76
scale pos weight	[0.0, 9.0]	1.71	1.55
max delta step	[0.0, 20.0]	13.78	8.38
subsample	[0.5, 1.0]	1.0	0.82
eta	[0.01, 0.05]	0.01	0.01
alpha	[0.0, 1.0]	0.40	0.62
lambda	[0.0, 10.0]	9.70	6.76
max depth	[3, 20]	20	20
gamma	[0.0, 10.0]	0.0	3.13
max bin	[10, 512]	286	56
Scale factor	Range	Value for Low Mass BDT	Value for High Mass BDT
SM ggF HH	[1, 200]	F	128.06
SM VBF HH	[1, 200]	-	15.44
ggF HH $\kappa_{\lambda} = 10$	[1, 200]	83.74	-
ggF HH $\kappa_{\lambda} = 5$	[1, 200]	1.0	-
VBF HH $\kappa_{\lambda} = 0$, $\kappa_{2V} = 1$, $\kappa_{V} = 1$	[1, 200]	1.0	5.43
VBF HH $\kappa_{\lambda} = 1$, $\kappa_{2V} = 1.5$, $\kappa_{V} = 1$	[1, 200]	27.65	56.06
VBF HH $\kappa_{\lambda} = 1$, $\kappa_{2V} = 3$, $\kappa_{V} = 1$	[1, 200]	1.0	1.0
VBF HH $\kappa_{\lambda} = -5$, $\kappa_{2V} = 1$, $\kappa_{V} = 0.5$	[1, 200]	68.45	1.0
VBF HH $\kappa_{\lambda} = 10$, $\kappa_{2V} = 1$, $\kappa_{V} = 1$	[1, 200]	118.76	1.0
$\gamma\gamma$ +jets	[1, 200]	183.72	194.15
$t\bar{t}H$	[1,100]	1.0	44.81
$ggH + b\bar{b}H$	[1,100]	1.0	38.65
$qq \rightarrow ZH + gg \rightarrow ZH$	[1,100]	1.0	3.61

Feature importance

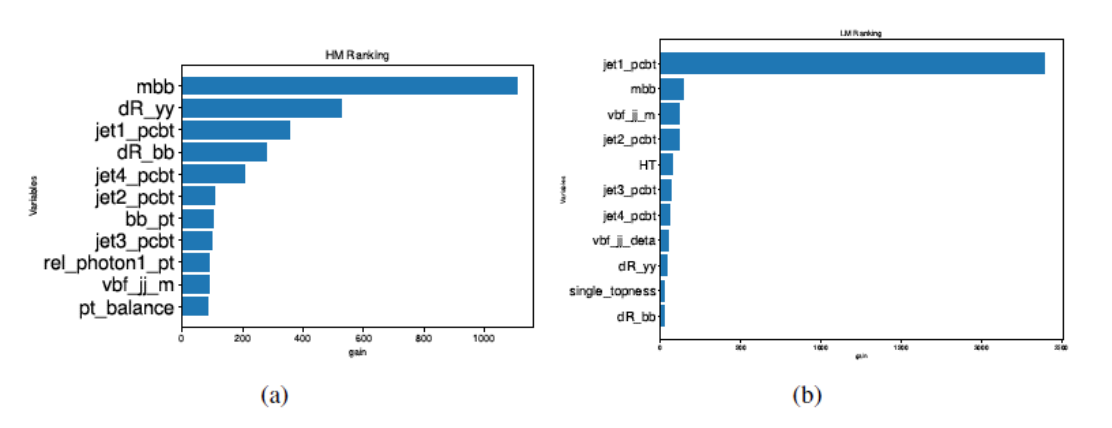


Figure 19: Feature importances for BDTs trained in the High Mass (left) and Low Mass (right) regions for the Run 2+3 dataset. The importance is measured using "gain", which quantifies how much the feature contributes to reducing the log loss.

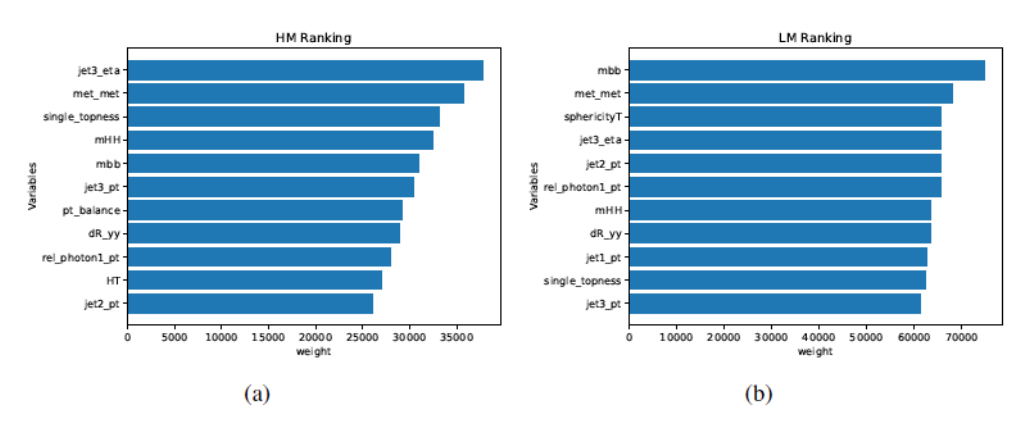


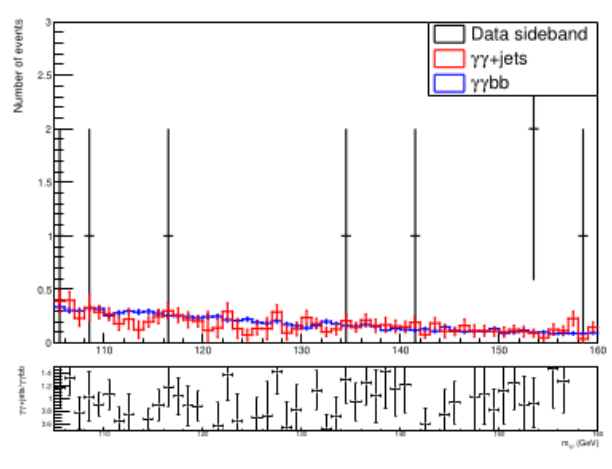
Figure 20: Feature importances for BDTs trained in the High Mass (left) and Low Mass (right) regions for the Run 2+3 dataset. The importance is measured using "split", which quantifies how many times the variable is used in the BDT training to separate signal from background.

Spurious signal test

- The spurious signal test is used to select the function form to describe the non-resonant background and estimate the bias as a system uncertainty on signal yield.
- The spurious signal test procedure :
 - Using non-resonant $\gamma \gamma + bb$ sample as template due to higher statistic.
 - Fit the background-only template using a signal+background model (exponential v.s. power: The exponential and power functions perform similarly and for simplicity the exponential function is chosen for all categories).
 - Perform multiple fits for $m_{\gamma\gamma} \in [123,127]~GeV$ in 0.5 GeV intervals.
 - The spurious signal N_{sp} , is defined as the Maximum fitted signal events in the 4GeV window.

Category	Function	N_{sp}	$\max(N_{sp}/\sigma_{bkg})$ [%]	$\max(\zeta_{sp})$ [%]	$\max(N_{sb}/S_{ref,SM})$	$\operatorname{Prob}(\chi^2)$ [%]
HM_3	Exponential	0.0421	3.46	0	3.11	66.4
HM_2	Exponential	-0.055	-3.56	0	-9.04	67.5
HM_1	Exponential	-0.149	-4.13	0	-16.4	22.2
LM_4	Exponential	0.108	6.2	0	292	67.2
LM_3	Exponential	-0.242	-10.8	0	-489	79.4
LM_2	Exponential	-0.447	-11.5	0	-439	87.7
LM_1	Exponential	-1.27	-18.1	-3.61	-909	17.3

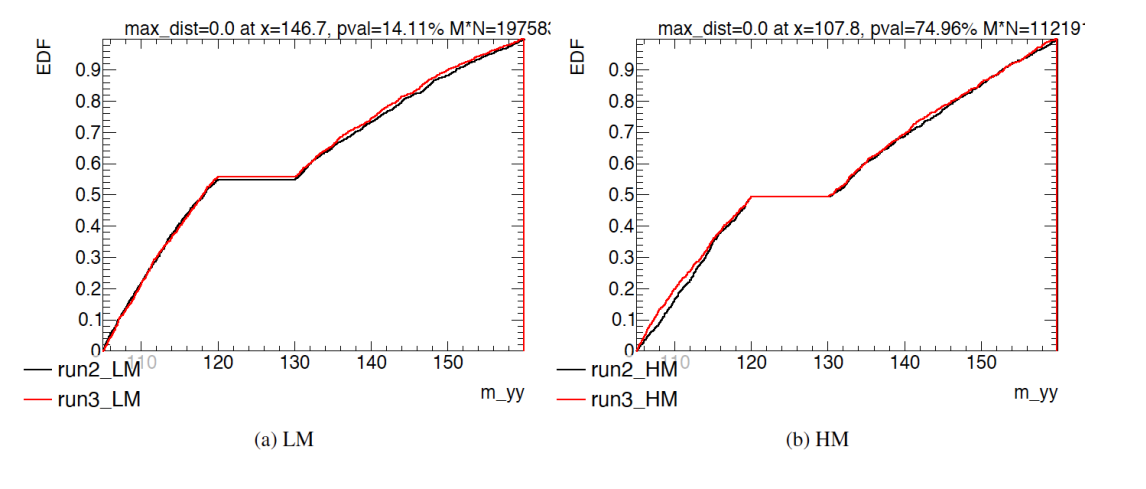
Table 26: Spurious signal for the exponential function evaluated on the $\gamma\gamma$ + HF sample, for the correlated model including 2024. The table shows: N_{sp} , the fitted spurious signal; $\max(N_{sp}/\sigma_{bkg})$, the maximum spurious signal divided by the expected fit uncertainty; $\max(\zeta_{sp})$, the maximum spurious signal divided by the expected fit uncertainty accounting for 2σ fluctuations in the MC template; and $\operatorname{Prob}(\chi^2)$, the χ^2 probability of the function from a background-only fit.



(c) Run 2 + Run 3 High Mass 3

Checks on background modelling strategy

- Compatibility test between Run2 and Run3 on data
 - Unbinned KS(Kolmogorov-Smirnov) test on data sideband for HM and LM region .
 - P-value :0.14 and 0.75 for LM and HM region .



- Checks the impact from the potential slope bias on final results
 - Bias= $\pm 10 \times |slope_{run2} slope_{run3}|$
 - Negligible impact on statistical result

Bias in shape	Run2=Run3	Run2=Run3+Bias	Run2=Run3-Bias	
Significance from fitting	1.047	1.045	1.052	
Upper limit on μ	2.369	2.370	2.364	

Table 28: Background shape bias check [61]. By alternating the background shape difference between Run2 and Run3 in each category pair, this introduces negligible changes in the statistical result.

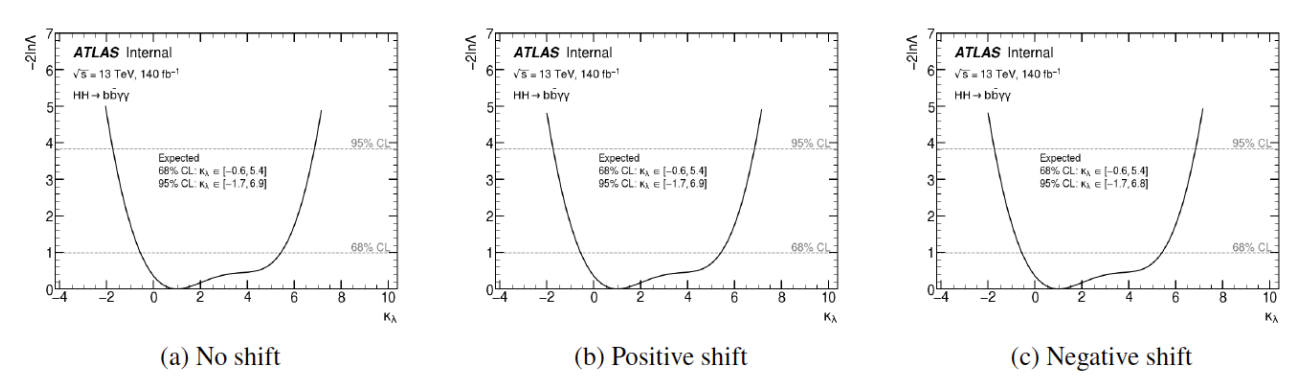


Figure 42: Background shape bias check effect on κ_{λ} limit

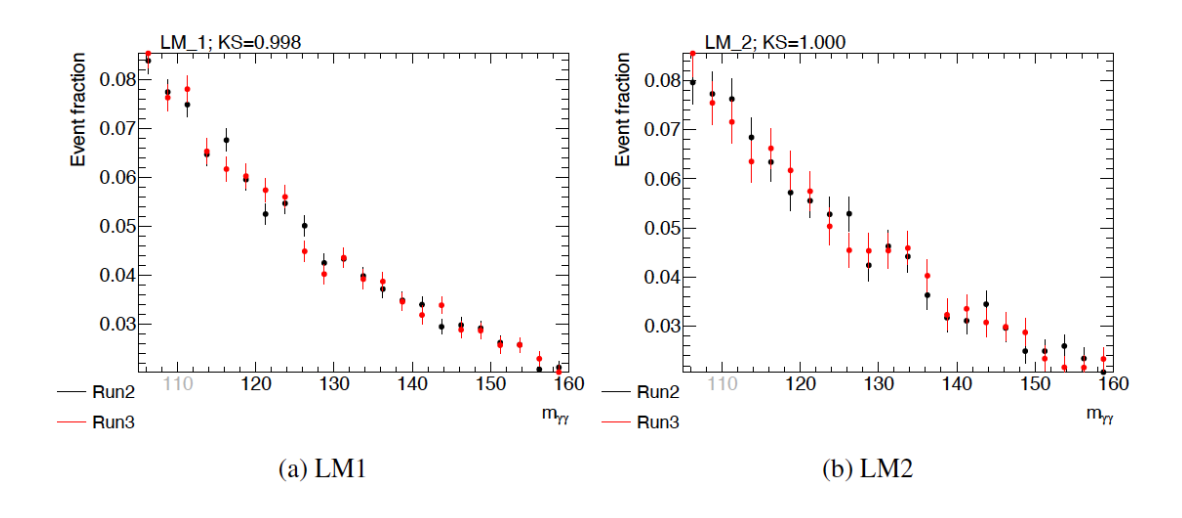
Checks on background modelling strategy

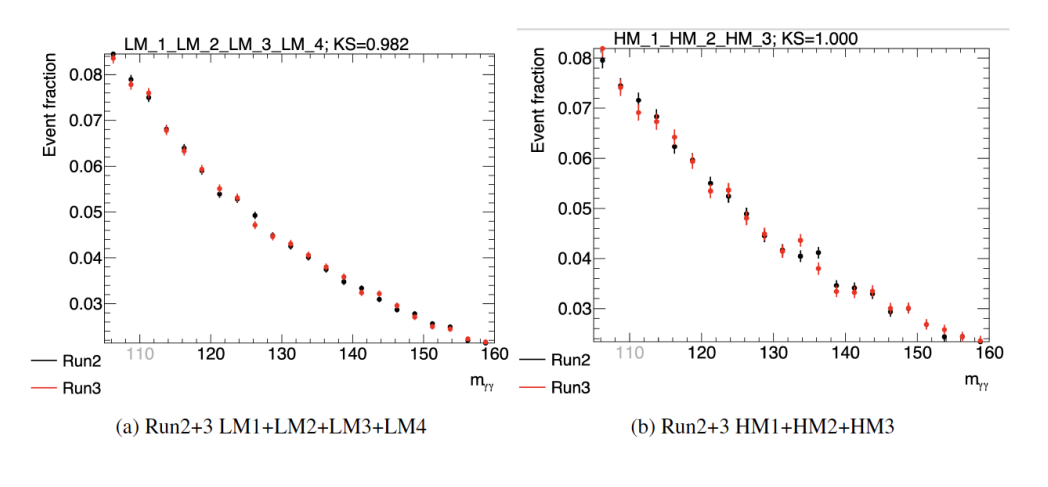
- Compatibility test between run2 and run3 on background shape
 - Using high stats $\gamma\gamma$ +bb sample.
 - Hypothesis testing with unbinned NLL: same shape(Null hypothesis) vs different shape(alternative hypothesis).

	LM1	LM2	LM3	LM4	HM1	HM2	HM3
Run2	2.599±0.030	2.647±0.050	2.920±0.092	2.748±0.106	2.338±0.045	2.547±0.091	2.611±0.111
Run3	2.566 ± 0.033	2.676 ± 0.055	2.711 ± 0.095	3.017 ± 0.117	2.343 ± 0.049	2.460 ± 0.097	2.517 ± 0.115
Correlated	2.581 ± 0.022	2.663 ± 0.038	2.803 ± 0.067	2.897 ± 0.080	2.342 ± 0.034	2.499 ± 0.067	2.558 ± 0.081
$\frac{2\Delta NLL}{NDOF}$	0.55429	0.15909	2.49586	2.86133	0.00685	0.42782	0.34120
p-value[%]	45.7	69.0	11.4	9.1	93.4	51.3	55.9

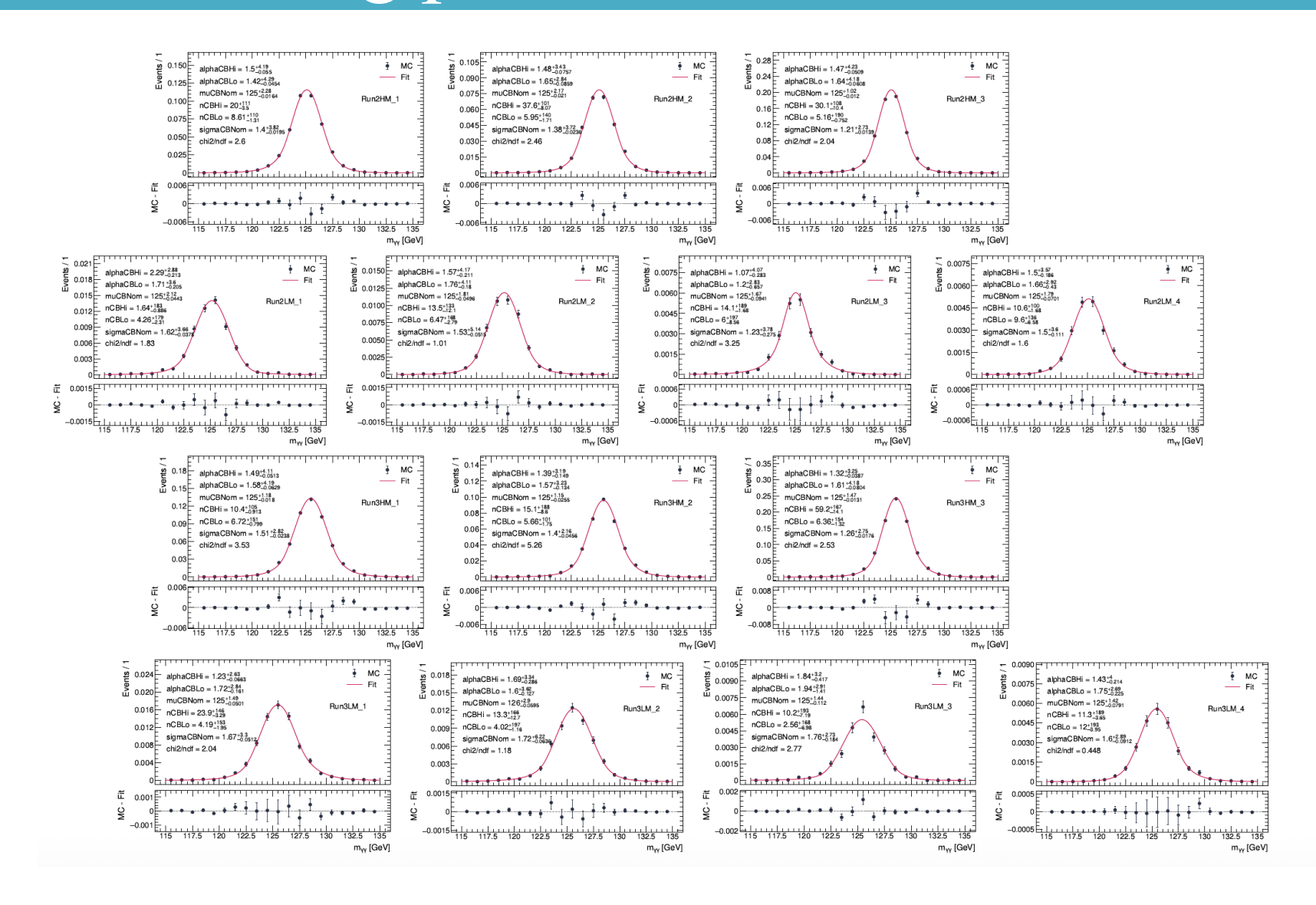
	LM1_LM2_LM3_LM4	HM1_HM2_HM3
Run2	2.639±0.024	2.410±0.038
Run3	2.622±0.026	2.395 ± 0.041
Correlated	2.629 ± 0.018	2.402 ± 0.028
$\frac{2\Delta NLL}{NDOF}$	0.19925	0.07364
p-value [%]	65.5	78.6

Table 25: Background shape (exponential β term) compatibility check with $\gamma\gamma b\bar{b}$ sample [61]. The first three rows show the slope (multiplied by 100) of the exponential function fitted for Run 2, Run 3 and Run 2+Run 3 correlation startegy. The large p-value indicates that the "same shape" hypothesis can not be rejected.





Signal Modelling plots



Signal Yield parametrization

The differential signal HH cross sections , and hence the respective yields, can be expressed as a polynomial of the coupling modifiers - κ_{λ} for ggF and $(\kappa_{\lambda}, \kappa_{2V}, \kappa_{V})$ for VBF - by performing a linear combination of the relevant simulated samples.

$$\begin{split} \frac{d\sigma_{ggF}}{d\Phi}(\kappa_{\lambda}) &= \left[\left(1 + \frac{1}{5} \kappa_{\lambda}^2 - \frac{6}{5} \kappa_{\lambda} \right) \cdot \frac{d\sigma_{ggF}}{d\Phi}(0, 1) \right. \\ &+ \left(\frac{5}{4} \kappa_{\lambda} - \frac{1}{4} \kappa_{\lambda}^2 \right) \cdot \frac{d\sigma_{ggF}}{d\Phi}(1, 1) \\ &+ \left(\frac{1}{20} \kappa_{\lambda}^2 - \frac{1}{20} \kappa_{\lambda} \right) \cdot \frac{d\sigma_{ggF}}{d\Phi}(5, 1) \right] \end{split}$$

$$\begin{split} \frac{d\sigma_{VBF}}{d\Phi}(\kappa_{\lambda},\kappa_{2V},\kappa_{V}) &= \left(\frac{68}{135}\kappa_{2V}^{2} + \frac{20}{27}\kappa_{2V}\kappa_{\lambda}\kappa_{V} - 4\kappa_{2V}\kappa_{V}^{2} + \frac{1}{9}\kappa_{\lambda}^{2}\kappa_{V}^{2} - \frac{56}{27}\kappa_{\lambda}\kappa_{V}^{3} + \frac{772}{135}\kappa_{V}^{4}\right) \cdot \frac{d\sigma_{VBF}}{d\Phi}(1,1,1) \\ &+ \left(-\frac{4}{5}\kappa_{2V}^{2} + 4\kappa_{2V}\kappa_{V}^{2} - \frac{16}{5}\kappa_{V}^{4}\right) \cdot \frac{d\sigma_{VBF}}{d\Phi}(1,1.5,1) \\ &+ \left(\frac{11}{60}\kappa_{2V}^{2} - \frac{19}{24}\kappa_{2V}\kappa_{\lambda}\kappa_{V} + \frac{1}{3}\kappa_{2V}\kappa_{V}^{2} - \frac{1}{8}\kappa_{\lambda}^{2}\kappa_{V}^{2} + \frac{13}{6}\kappa_{\lambda}\kappa_{V}^{3} - \frac{53}{30}\kappa_{V}^{4}\right) \cdot \frac{d\sigma_{VBF}}{d\Phi}(2,1,1) \\ &+ \left(-\frac{11}{540}\kappa_{2V}^{2} + \frac{11}{216}\kappa_{2V}\kappa_{\lambda}\kappa_{V} + \frac{1}{72}\kappa_{\lambda}^{2}\kappa_{V}^{2} - \frac{5}{54}\kappa_{\lambda}\kappa_{V}^{3} + \frac{13}{270}\kappa_{V}^{4}\right) \cdot \frac{d\sigma_{VBF}}{d\Phi}(10,1,1) \\ &+ \left(\frac{88}{45}\kappa_{2V}^{2} + \frac{4}{9}\kappa_{2V}\kappa_{\lambda}\kappa_{V} - \frac{16}{3}\kappa_{2V}\kappa_{V}^{2} - \frac{4}{9}\kappa_{\lambda}\kappa_{V}^{3} + \frac{152}{45}\kappa_{V}^{4}\right) \cdot \frac{d\sigma_{VBF}}{d\Phi}(1,1,0.5) \\ &+ \left(\frac{8}{45}\kappa_{2V}^{2} - \frac{4}{9}\kappa_{2V}\kappa_{\lambda}\kappa_{V} + \frac{4}{9}\kappa_{\lambda}\kappa_{V}^{3} - \frac{8}{45}\kappa_{V}^{4}\right) \cdot \frac{d\sigma_{VBF}}{d\Phi}(-5,1,0.5) \end{split}$$

Disagreements between the reweighting formula and directly generated samples are taken into account by creating systematic uncertainties.

Parameterization uncertainties

ggF(%)	HM_1	HM_2	HM_3	LM_1	LM_2	LM_3	LM_4
Run2	7.33 ± 2.76	5.00 ± 4.09	8.45 ± 2.88	4.20 ± 2.92	12.67 ± 3.03	6.82 ± 5.06	10.25 ± 6.59
Run3	12.50 ± 2.81	5.89 ± 2.75	5.37 ± 2.81	11.15 ± 3.18	7.26 ± 3.28	22.90 ± 4.09	10.84 ± 6.24
VBF(%)	HM_1	HM_2	HM_3	LM_1	LM_2	LM_3	LM_4
Run2	1.75 ± 1.10	2.90 ± 0.82	2.11 ± 0.77	4.66 ± 3.11	8.46 ± 2.42	6.50 ± 2.43	5.99 ± 1.52
Run3	9.68 ± 4.03	7.31 ± 4.59	6.76 ± 1.68	24.28 ± 6.78	28.80 ± 7.46	15.47 ± 15.13	9.94 ± 5.30

Systematic Uncertainties

Syste	Systematic uncertainties relevant for resonant backgrounds								
		ggF HH	VBF HH	Single HH					
Theory	and branching fraction \bullet PDF + α_S \bullet Scale + m_{top}		• BR($\gamma\gamma$) and BR($b\bar{b}$) • PDF + α_S • Scale + m _{top}	 BR(γ γ) Heavy flavour unc (100% only for ggF, VBF, WH) 					
	Acceptance/	ggF HH parametrisation	VBF HH parametrisation						
	Yields	Scale, PDF + α_{S} , Parton shower							
Exp.	Yields	 Photon ID and iso efficier Photon energy scale and Jet energy scale and resc JVT and fJVT efficiency Flavour tagging efficiency 	* Luminosity						
	Shape	Photon energy scalePhoton energy resolution							

Systematic uncertainty relevant for continuum background

Spurious signal uncertainty calculated by fits to $\gamma\gamma$ +bb MC sample. Small impact, e.g. N_{sp} ~ -0.149 in HM1.

Following CP recommendations:

Trigger: 4%(8%) for 2022 (2023-2024)

Lumi: 4% for 2022-2023 (2024)

Correlation scheme:

Trigger: 2022 decorr due to L1 trigger change.

Lumi: 2024 decorrelated (no measurement)

 JetEtMiss: correlate Run 2/3 except in-situ non closure and AF3/FullSim

Muon, theory, spurious: fully correlated

Rest experimental NPs uncorrelated.

Extrapolation to 2024 dataset:

 FTAG uncertainties have negligible impact, apply 2022+2023 to 2024

 Trigger efficiency uncertainty doubled for 2023-2024

Systematic breakdown

- Evaluate the impact on 95 % μ_{HH} upper limit
- Floating a group of systematics while fixing others to 0,then compare to the stat only result

Course of exetematic uncertainty	Relative impact [%		
Source of systematic uncertainty	Up	Down	
Experimental			
Photon energy scale	+20	-30	
Photon energy resolution	+13	-6.8	
Photon efficiency	+13	-2.5	
Jet	+9.6	-6.4	
Luminosity	+6.3	-1.1	
Theory			
QCD scale + m_{top} , PDF+ α_S	+34	-4.5	
$\mathcal{B}(H \to \gamma \gamma, b \bar{b})$	+9.9	-2.1	
Parton showering model	±	15	
Heavy-flavour content	±2	29	
Background model			
Spurious signal	土	6.5	

NP Ranking Plots

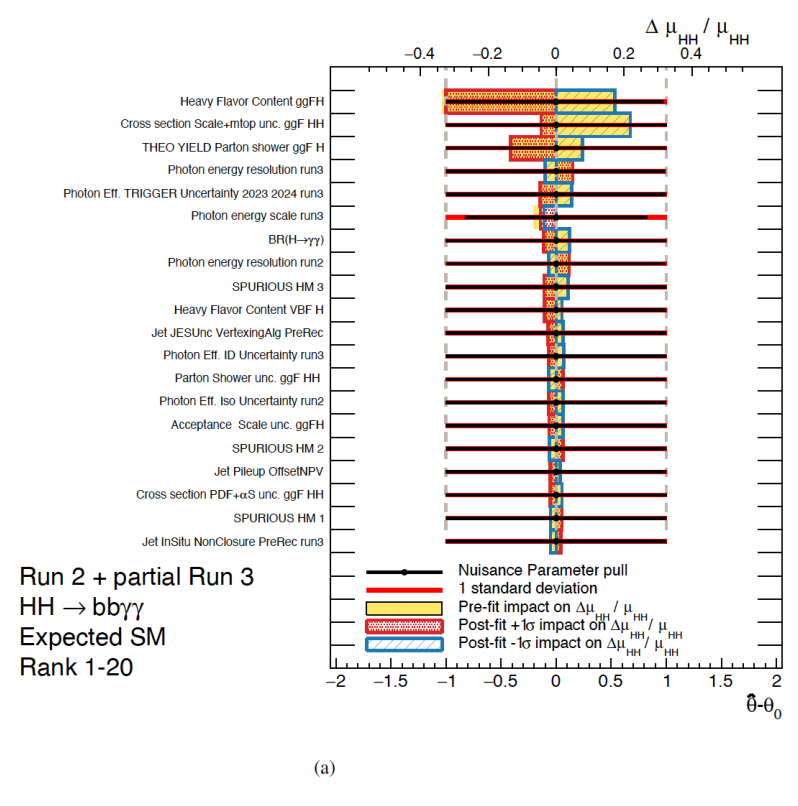


Figure 69: The expected impacts of the systematic uncertainties on the μ_{HH} measurement.

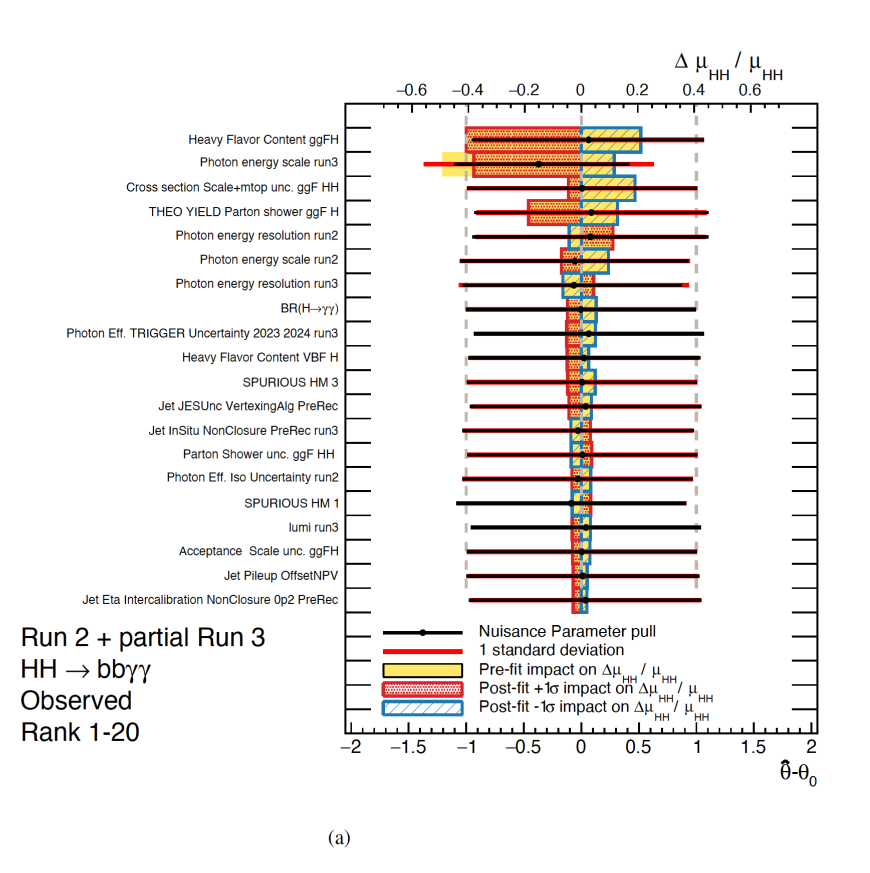
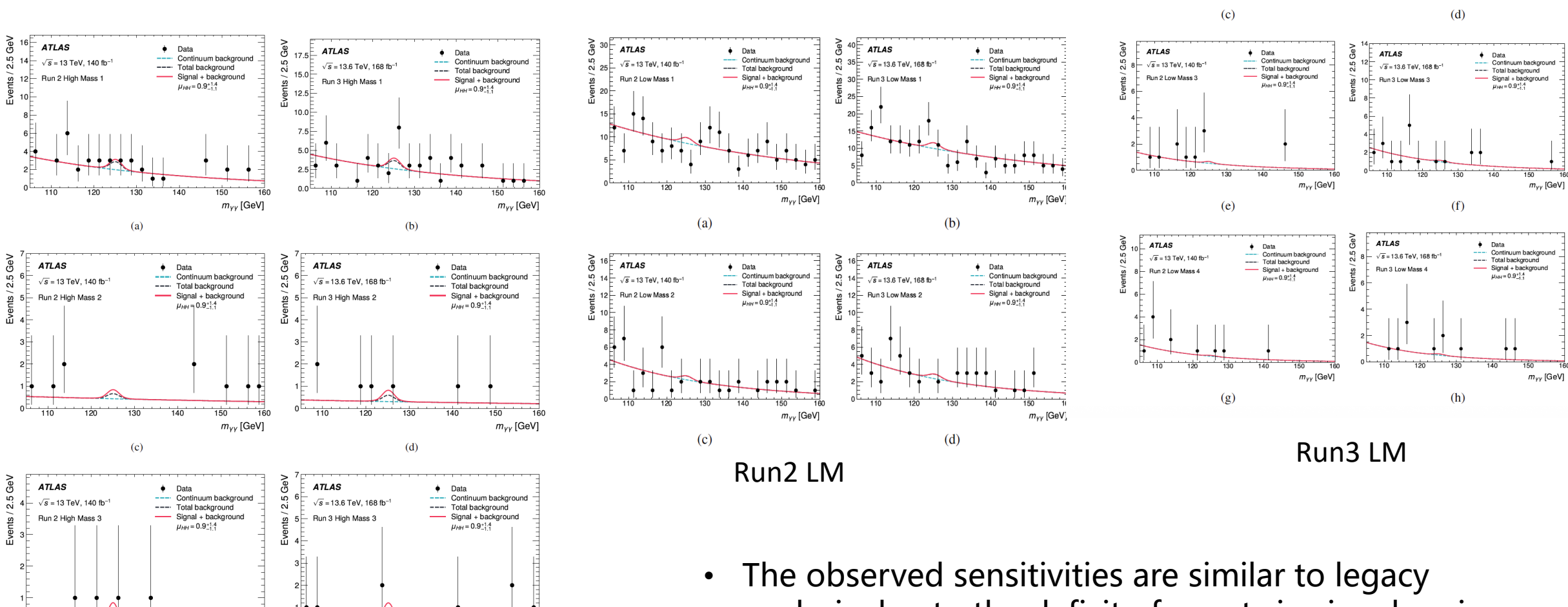


Figure 70: The observed impacts of the systematic uncertainties on the μ_{HH} measurement.

Fit Plots



Run2 HM

130

(e)

 $m_{\gamma\gamma}$ [GeV]

120

Run3 HM

(f)

analysis due to the deficit of events in signal region.

2025/10/31 31

 $m_{\gamma\gamma}$ [GeV]

Post-fit yields

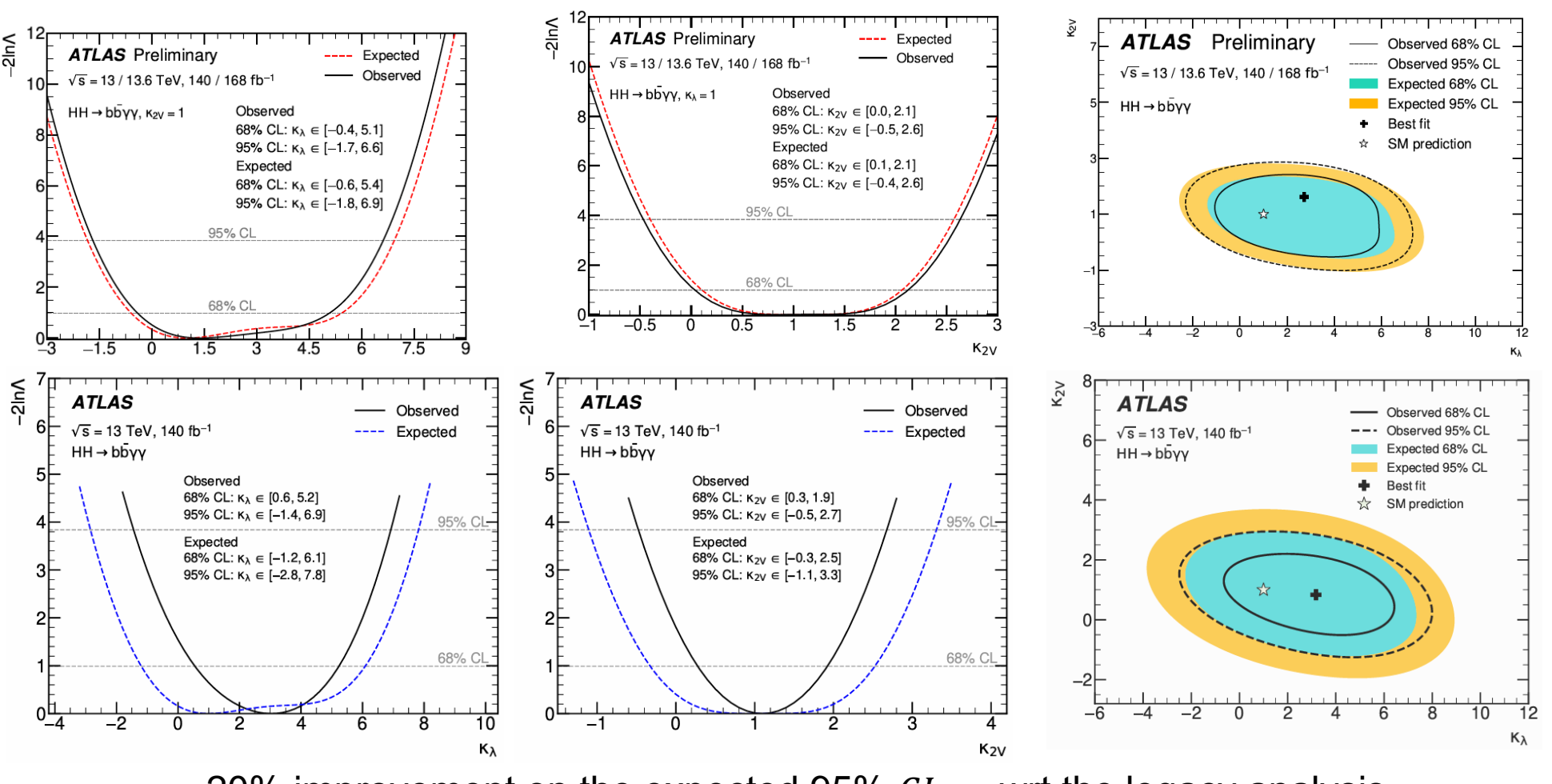
	HM 1	HM 2	HM 3	LM 1	LM 2	LM 3	LM 4
SM HH signal	$0.41^{+0.04}_{-0.07}$	$0.28^{+0.03}_{-0.04}$	$0.66^{+0.07}_{-0.11}$	$0.058^{+0.012}_{-0.006}$	$0.043^{+0.009}_{-0.005}$	$0.021^{+0.004}_{-0.003}$	0.019+0.003
ggF $(\kappa_{\lambda} = 1)$	$0.40^{+0.04}_{-0.07}$	$0.27^{+0.03}_{-0.04}$	$0.64^{+0.07}_{-0.10}$	$0.055^{+0.011}_{-0.006}$	$0.040^{+0.009}_{-0.004}$	$0.019^{+0.004}_{-0.003}$	$0.013^{+0.003}_{-0.002}$
$\text{VBF}\left(\kappa_{\lambda}=1\right)$	$0.012^{+0.001}_{-0.001}$	$0.007^{\tiny{+0.001}}_{\tiny{-0.000}}$	$0.021^{+0.002}_{-0.001}$	$0.003^{+0.000}_{-0.000}$	$0.002^{+0.000}_{-0.000}$	$0.002^{+0.000}_{-0.000}$	$0.006^{+0.000}_{-0.000}$
Alternative BSM HH signals							
ggF HH ($\kappa_{\lambda} = 5$)	$0.33^{+0.07}_{-0.05}$	$0.17^{+0.04}_{-0.03}$	$0.30^{+0.07}_{-0.05}$	$0.95^{+0.16}_{-0.17}$	$0.68^{+0.15}_{-0.14}$	$0.28^{+0.05}_{-0.05}$	$0.22^{+0.04}_{-0.04}$
VBF HH ($\kappa_{\lambda} = 10$)	$0.38^{+0.03}_{-0.03}$	$0.28^{+0.02}_{-0.02}$	$1.03^{+0.08}_{-0.08}$	$0.38^{+0.05}_{-0.04}$	$0.40^{+0.05}_{-0.05}$	$0.34^{+0.05}_{-0.04}$	$1.40^{+0.15}_{-0.13}$
$VBF HH (\kappa_{2V} = 3)$	$0.41^{+0.03}_{-0.03}$	$0.32^{+0.03}_{-0.02}$	$3.7^{+0.3}_{-0.3}$	$0.042^{+0.006}_{-0.005}$	$0.043^{+0.006}_{-0.005}$	$0.037^{+0.005}_{-0.004}$	$0.159^{+0.017}_{-0.015}$
Single Higgs boson background	1.3+0.4	0.33+0.18	0.30+0.18 -0.09	2.1+0.4 -0.3	0.71+0.12 -0.08	0.19+0.04 -0.02	0.10+0.07 -0.02
ggH	$0.4^{+0.4}_{-0.2}$	$0.14^{+0.17}_{-0.08}$	$0.18^{+0.18}_{-0.09}$	$0.28^{+0.30}_{-0.17}$	$0.10^{+0.10}_{-0.05}$	$0.027^{+0.030}_{-0.013}$	$0.018^{+0.070}_{-0.019}$
$tar{t}H$	$0.22^{+0.03}_{-0.03}$	$0.045^{+0.010}_{-0.008}$	$0.027^{+0.005}_{-0.005}$	$1.10^{+0.13}_{-0.12}$	$0.39^{+0.05}_{-0.05}$	$0.098^{+0.012}_{-0.012}$	$0.035^{+0.005}_{-0.005}$
ZH	$0.47^{+0.07}_{-0.06}$	$0.091^{+0.020}_{-0.018}$	$0.064^{+0.011}_{-0.009}$	$0.41^{+0.06}_{-0.06}$	$0.12^{+0.03}_{-0.02}$	$0.032^{+0.012}_{-0.009}$	$0.014^{+0.004}_{-0.003}$
Other <i>H</i>	$0.19^{+0.06}_{-0.04}$	$0.046^{+0.017}_{-0.010}$	$0.031^{+0.020}_{-0.012}$	$0.28^{+0.05}_{-0.04}$	$0.101^{+0.018}_{-0.014}$	$0.035^{+0.007}_{-0.005}$	$0.037^{+0.005}_{-0.005}$
Continuum background	$8.0^{+1.2}_{-1.4}$	$1.7^{+0.6}_{-0.6}$	$0.5^{+0.3}_{-0.3}$	34+3	$8.9^{+1.4}_{-0.3}$	$2.1^{+0.7}_{-0.6}$	$2.1^{+0.7}_{-0.7}$
Total background	$9.2^{+1.3}_{-1.4}$	$2.1^{+0.6}_{-0.6}$	$0.8^{+0.4}_{-0.3}$	37 +3	$9.6^{+1.4}_{-1.3}$	$2.3^{+0.7}_{-0.6}$	$2.2^{+0.7}_{-0.7}$
——————————————————————————————————————	12	0	2	28	5	4	3

	HM 1	HM 2	HM 3	LM 1	LM 2	LM 3	LM 4
SM HH signal	$0.54^{+0.08}_{-0.08}$	$0.35^{+0.05}_{-0.06}$	$0.84^{+0.13}_{-0.14}$	$0.072^{+0.015}_{-0.010}$	$0.054^{+0.013}_{-0.009}$	$0.027^{+0.006}_{-0.005}$	$0.025^{+0.006}_{-0.005}$
ggF $(\kappa_{\lambda} = 1)$	$0.53^{+0.08}_{-0.08}$	$0.34^{+0.05}_{-0.06}$	$0.81^{+0.13}_{-0.14}$	$0.069^{+0.015}_{-0.010}$	$0.050^{+0.013}_{-0.009}$	$0.024^{+0.006}_{-0.004}$	$0.017^{+0.005}_{-0.004}$
$\text{VBF}\left(\kappa_{\lambda}=1\right)$	$0.015^{+0.002}_{-0.001}$	$0.009^{+0.001}_{-0.001}$	$0.026^{+0.003}_{-0.003}$	$0.003^{+0.001}_{-0.000}$	$0.003^{+0.001}_{-0.001}$	$0.002^{+0.000}_{-0.000}$	$0.008^{+0.002}_{-0.001}$
Alternative BSM HH signals							
ggF HH ($\kappa_{\lambda} = 5$)	$0.42^{+0.12}_{-0.08}$	$0.22^{+0.05}_{-0.04}$	$0.39^{+0.10}_{-0.06}$	$1.2^{+0.3}_{-0.2}$	$0.83^{+0.20}_{-0.16}$	$0.38^{+0.12}_{-0.10}$	$0.30^{+0.09}_{-0.07}$
VBF HH ($\kappa_{\lambda} = 10$)	$0.50^{+0.08}_{-0.06}$	$0.36^{+0.05}_{-0.04}$	$1.19^{+0.18}_{-0.15}$	$0.48^{+0.15}_{-0.11}$	$0.53^{+0.18}_{-0.13}$	$0.43^{+0.10}_{-0.10}$	$1.8^{+0.5}_{-0.3}$
$VBF HH (\kappa_{2V} = 3)$	$0.57^{+0.09}_{-0.07}$	$0.44^{+0.06}_{-0.06}$	$4.9^{+0.8}_{-0.6}$	$0.052^{+0.017}_{-0.012}$	$0.048^{+0.017}_{-0.012}$	$0.049^{+0.012}_{-0.011}$	$0.19^{+0.05}_{-0.04}$
Single Higgs boson background	1.6+0.7	0.40+0.18	0.36+0.27 -0.12	2.7+0.8 -0.5	0.89+0.20 -0.14	0.26+0.10 -0.05	$0.16^{+0.08}_{-0.04}$
ggH	$0.5^{+0.7}_{-0.3}$	$0.15^{+0.17}_{-0.08}$	$0.18^{+0.27}_{-0.11}$	$0.6^{+0.7}_{-0.4}$	$0.15^{+0.17}_{-0.08}$	$0.06^{+0.10}_{-0.04}$	$0.04^{+0.06}_{-0.03}$
$t\bar{t}H$	$0.29^{+0.06}_{-0.06}$	$0.053^{+0.016}_{-0.014}$	$0.030^{+0.021}_{-0.013}$	$1.42^{+0.20}_{-0.17}$	$0.52^{+0.07}_{-0.07}$	$0.12^{+0.02}_{-0.02}$	$0.051^{+0.009}_{-0.008}$
ZH	$0.60^{+0.12}_{-0.10}$	$0.13^{+0.05}_{-0.04}$	$0.098^{+0.021}_{-0.017}$	$0.47^{+0.10}_{-0.08}$	$0.14^{+0.04}_{-0.03}$	$0.039^{+0.022}_{-0.013}$	$0.018^{+0.030}_{-0.013}$
Other <i>H</i>	$0.23^{+0.10}_{-0.05}$	$0.069^{+0.019}_{-0.011}$	$0.050^{+0.023}_{-0.012}$	$0.29^{+0.06}_{-0.05}$	$0.080^{+0.020}_{-0.013}$	$0.043^{+0.012}_{-0.007}$	$0.048^{+0.021}_{-0.010}$
Continuum background	$10.4^{+1.4}_{-1.5}$	$1.2^{+0.5}_{-0.5}$	$1.3^{+0.6}_{-0.5}$	40^{+3}_{-3}	$9.5^{+1.4}_{-1.4}$	$3.9^{+0.9}_{-0.9}$	$2.1_{-0.6}^{+0.7}$
Total background	$11.9^{+1.5}_{-1.5}$	$1.6^{+0.5}_{-0.5}$	$1.7^{+0.6}_{-0.5}$	43^{+3}_{-3}	$10.4^{+1.4}_{-1.4}$	$4.2^{+0.9}_{-0.9}$	$2.2^{+0.7}_{-0.6}$
Data	16	2	2	46	4	2	3

Run2 Run3

• The observed sensitivities are similar to legacy analysis due to the deficit of events in signal region.

Results compare to legacy



New results

Old results in legacy run2

- ~20% improvement on the expected 95% $CL \kappa_{\lambda}$ wrt the legacy analysis
- ~30% improvement on the expected 95% $CL \kappa_{2V}$ wrt the legacy analysis
- Smaller improvement as expected due to the Powheg bug fix, Smaller ggFHH Xsec and VBFHH Xec.